DELIVERY OF RETINOIC ACID UTILIZING CELL PENETRATING PEPTIDES IN HUMAN NEUROBLASTOMA CELLS

A Thesis
Submitted to
the Temple University Graduate Board

In Partial Fulfillment
of the Requirements for the Degree
MASTER'S OF SCIENCE IN BIOENGINEERING

By
Liam P. Kelly
Diploma Date: May 2019

Thesis Approvals:

Dr. Won Suh, Advisory Chair, Bioengineering
Dr. Peter Lelkes, Bioengineering
Dr. Karin Wang, Bioengineering

ABSTRACT

Cancer is the second leading cause of death in America. In 2018, there were 9.5 million deaths due to cancer according to the International Agency for Research on Cancer (IARC), and this number is expected to grow to 16.3 million by 2040. Among the type of cancers, neuroblastoma and nerve tissue cancers have a 5-year survival rate of 33%, which is very low. One of the main issues linked to such situations is due to the lack of specificity in removing tumor cells. While clinical therapies work to reduce tumor mass as much as possible, they cannot always target all of them, and once some cancer cells are left behind, they regrow and spread. The work of this thesis seeks to enhance the treatment outcome by utilizing all-*trans* retinoic acid (ATRA), a metabolite of vitamin A, to induce differentiation of nerve tissue cancer cells and eliminate their ability to self-renew (reemerge). Differentiation therapy is currently utilized in select clinical applications but the utilization of ATRA is limited due to its poor solubility in the blood, low bioavailability, short half-life, and *in vivo* toxicity. In order to alleviate some of these issues, the ATRA molecule was engineered with a novel cell penetrating peptide and tested for its efficacy. Data and results presented herein report the differentiation induced by the CPP-conjugated ATRA may act as a viable method for neuroblastoma treatment.

TABLE OF CONTENTS

LIST OF TABLES

Page

LIST OF FIGURES

1. INTRODUCTION & BACKGROUND

1.1. Neuroblastoma (Nerve Tissue Cancer)

Cancer is expensive, not only by the financial burden placed on patients but through the suffering it leaves behind. Between 2008 and 2012, global cases of cancer raised from 12.7 million to 14.1 million and is predicted to reach 25 million by 2030 [1]. Of these cases, nerve tissue cancers make up just 1.4% of all cancers, totaling around 250,000 people globally [1]. While only contributing to a small percentage, they disproportionately represent cancer's impact. With a 33.2% 5-year survival rate in the United States, they account for 2.8% of cancer deaths, making it the tenth leading cause of cancer-related death in the United States [2]. Cancer defines a class of diseases where an abnormal growth of cells accumulates over time. This growth leads to the formation of tumors, which continue to grow and possess the potential metastasize (i.e., spread) to other regions of the body. As it relates to nerve tissue cancers, such as neuroblastoma, there are two classes of tumors: cancerous and benign. This classification is chiefly defined by the growth of the tumor, i.e., cancerous tumors exhibit continual growth while benign tumors are a mass of lowly proliferative cells which lack the ability to spread or infect other cells. The aim, then, of cancer treatments is to eliminate these cancerous cells from a tumor so they no longer pose a threat to neighboring tissue.

Neuroblastoma is a single type of cancer that is present in the nervous tissue. It is the most common type of cancer in babies and is third in children after brain cancer and leukemia. In high-risk patients, the survival rate is as low as 40% [2]. Neuroblastoma tumors are composed of cells that exist in an undifferentiated state, which under normal physiology will continue to proliferate indefinitely [3]. It is this unique train of self-renewal that leads to tumorigenesis, coupled by its ability to differentiate into mature cells which create the majority of the tumor's mass [3]. Most modern approaches in cancer treatment (e.g., chemotherapy or radiation therapy) target cells that express some marker for differentiation [3], [4]. While effective in decreasing a tumor's size, these approaches only eliminate differentiated or differentiating cells, and fail to adequately target neuroblastomas. This is one of the reasons why after a patient goes into remission, they must continuously return to monitor their progress, so that to ensure no regrowth of the tumor occurs. Coupled by the problems associated with this treatment's specificity, there are numerous side effects that come from this poorly directed method, effecting normal,

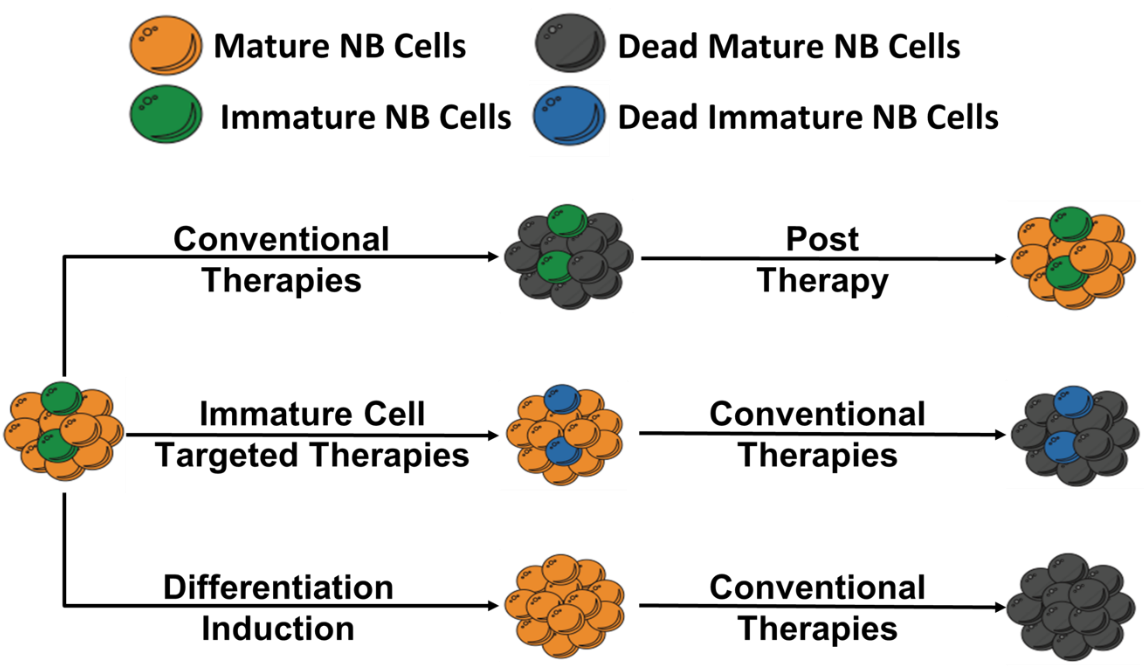

Figure 1. Development of Cancerous Tumors in Various Cancer Therapies

Conventional therapies for cancer treatment act by targeting differentiated cells, failing to eliminate the neuroblastoma causing the tumor growth, which results in eventual regrowth of tumor (Top). Modern methods to combat this problem by either eliminating undifferentiated neuroblastoma cells or by inducing differentiation (Bottom). Both approaches achieve the same result, elimination of undifferentiated cells. From here, conventional therapies are successful in removing tumor mass.

healthy cells. This has the potential to affect every part of the human system, including weight changes, hair loss, mood changes, kidney problems, nerve pain and fertility problems [4].

To combat the problems with conventional methods of treating tumors, newer techniques are being developed to directly target undifferentiated cancer cells. These methods function by either targeting and eliminating neuroblastomas, or by inducing differentiation of neuroblastomas into mature cells (Figure 1) [3]. Both methods yield the same outcome, an elimination of undifferentiated cells from the tumor, which ceases the growth of the tumor. With the cells responsible for generating the tumor mass removed, the neuroblastoma transitions into a benign tumor. From here, conventional methods of targeting differentiated cells shine, removing any remaining tumor cells. Herein will discuss the potential of the later method, differentiation of neuroblastoma, as a possibility for tumor treatment.

1.2. Retinoic Acid

Retinoic acid is a metabolite of vitamin A and is part of a widely researched class of molecules for cell growth and development. Specific to cancer treatment, retinoic acid has been used in a large array of studies to induce differentiation in cells [8]–[13]. The human body obtains retinoic acid through two sources, either in the form of Vitamin A (retinol) or as Provitamin A (β-carotene). While Vitamin A is abundant in certain foods, such as animals and animal products, Provitamin A is chiefly found in fruits and vegetables and needs to first be converted to retinol prior to retinoic acid synthesis. This conversion of provitamin A to retinol is mediated by dioxygenase, an enzyme found in the liver. Once in the form of retinol, the molecule diffuses into the cell, where it is oxidized into retinaldehyde by one of two classes of dehydrogenase/reductase: cytosolic alcohol dehydrogenases (ADHs) and retinol dehydrogenases (RDHs) [12]. The final oxidation from retinaldehyde to all-*trans* retinoic acid (ATRA)is carried out by three retinaldehyde dehydrogenases (RALDHs): RALDH1, RALDH2 and RALDH3 [12]. In the cytosol, ATRA binds with cellular retinoic acid binding proteins (CRABP). CRABP-2 facilitates the nuclear import of ATRA and the subsequent binding within the nucleus [12]. Here, dimers of retinoic acid receptors (RAR) and retinoid X receptors (RXR), termed

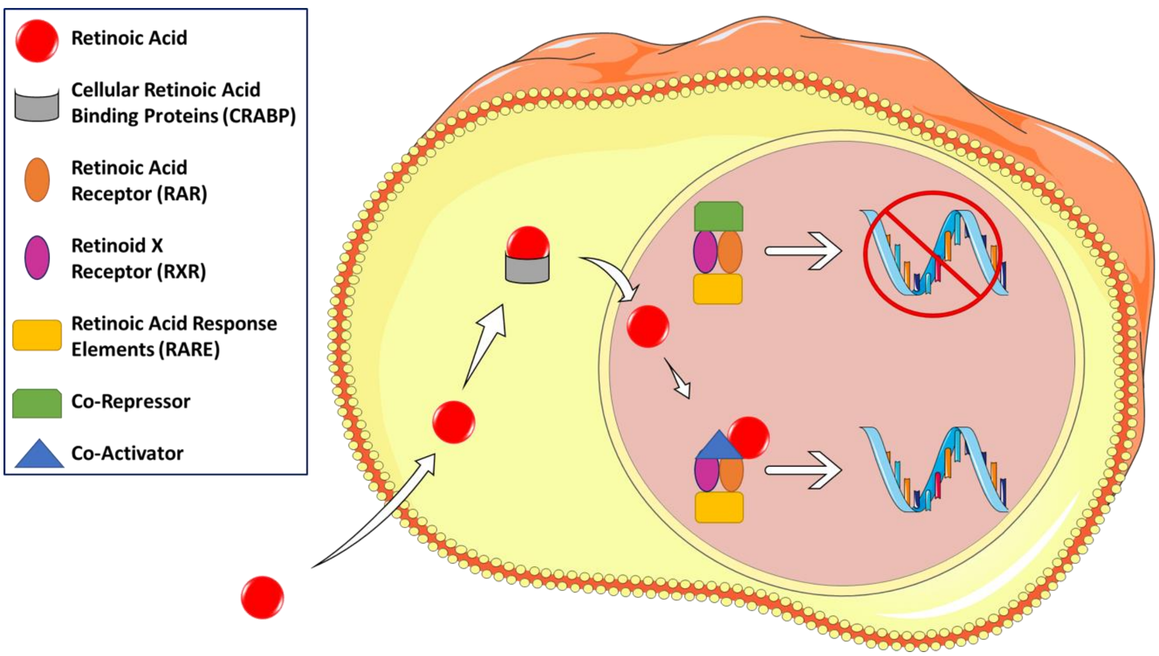

Figure 2. Retinoic Acid Intracellular Transcription Pathway

All-*trans* retinoic acid (ATRA) from the blood enters the cell through diffusion. Once in the cytosol, ATRA binds to cellular retinoic acid binding protein 2 (CRABP-2) which helps facilitate transport into the nucleus. Under normal physiology, retinoic acid receptors (RAR) and retinoid X receptors (RXR) located on retinoic acid response elements (RAREs) are bound to a co-repressor protein complex, which prevents transcription. Introduction of ATRA induces a conformational change to this system, removing the co-repressor and recruiting a co-activator, which signals a transcription complex that induces differentiation.

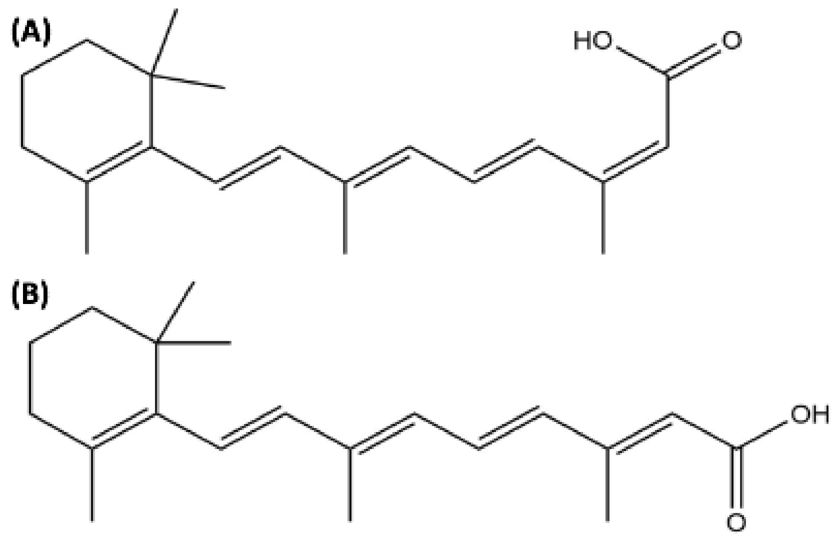

Figure 3. Retinoic Acid Chemical Isomer Structures

Two chemical structures of retinoic acid: (A) 13-cis Retinoic Acid (13cRA) and (B) All-trans Retinoic Acid (ATRA). The active form, ATRA, is capable of inducing differentiation however causes unintended cytotoxic effects in patients. In clinical applications, the inactive form 13cRA is administered and undergoes *cis-trans* isomerization within the cell's cytoplasm.

RAR/RXR, bind to specific retinoic acid response elements (RAREs) in the DNA [13]–[15]. Under normal conditions, protein complexes (co-repressors) stabilize the chromatin structure and prevent transcription [12]. Upon ATRA delivery, binding to RAR releases the co-repressor and recruits a co-activator protein complex [12]. This destabilization promotes a transcription complex related to cellular differentiation [14].

Currently, retinoic acid treatments are limited to use after treatments using a conventional therapy as a means to supplement the body during remission [16]. According to Clinicaltrials.gov, there are 28 current clinical trials looking at the use of retinoic acid as tumor treatment method, 7 of them specifically looking at neuroblastoma. Additionally, there are 60 completed trials treating tumors with 12 of them related specifically to neuroblastoma. There are two primary isomers of retinoic acid that are used for research and clinical applications, 13-*cis* retinoic acid (13cRA) and all-*trans* retinoic acid (ATRA)

(Figure 3). As it relates to pharmaceuticals, these isomers are commonly referred to as isotretinoin and tretinoin, respectively. While most research favors the use of ATRA, clinical applications preferentially utilize 13cRA to avoid the toxic effects ATRA has on cells [17], [18]. There are, however, drawbacks to using the 13cRA, namely its lower binding affinity to RAR/RXR domains [19]. Once in cells, the prodrug, 13cRA, undergoes intracellular cis-trans isomerization into ATRA, where it activates and subsequently binds to receptors [19]. This isomerization process helps protect the surrounding cells against the cytotoxic effects from the ATRA [17], [18].

While pharmaceuticals can deliver RA (13cRA or ATRA) to the body, there are many drawbacks which limits its efficacy. RA is highly hydrophobic, lending to its low solubility in aqueous environments (0.21 μM at pH 7.3) [20]. This results in a low absorption by the body, causing both poor bioavailability and gastrointestinal issues from the leftover RA [20]. Additionally, RA has a very short half-life (<1 hour) [5], complicating treatments by delivering a variable amount of drug. To combat these problems, multiple methods have been shown to deliver RA to cells, which include encapsulation in microspheres [8], nanoparticles [10], polymers [7], nanostructures [6] and cell penetrating peptides [21]. Specifically, for the purposes of this thesis, cell penetrating peptides will be utilized as a delivery mechanism.

1.3. Retinoic Acid Delivery

Cell penetrating peptides (CPPs) are short amino acid sequences (typically <20) that attach and facilitate uptake of a bioactive cargo. Despite the highly selective nature of cellular membranes, which prevents non-approved proteins, drugs and other molecules across, CPPs have the unique ability to bypass the cells border. The first molecule capable of this was discovered in 1988, derived from the trans-activator of transcription (TAT) protein found in HIV-1 [22], [23]. Years later, researchers found that the sequence responsible for translocating the membrane could be trimmed down from the original 86-mer to as short as 13 [24] or 9 [25] amino acids. Shortly after the discovery of TAT, another peptide was discovered in the Antennapedia protein homeodomain of *Drosophila* (60-mer) that exhibited similar penetration capabilities compared to TAT [26]. Researchers later discovered that only the third helix of this peptide (16-mer) is needed to be internalized by cells [27].

1.3.1. Cell Penetrating Peptide (CPP) Classes

As CPPs have become more widely studied, researchers have characterized three different classes: cationic, amphipathic (or amphiphilic), and hydrophobic [28]. Cationic CPPs, such as TAT, or Penetratin, make use of their overall positive charge to disrupt the negative membrane potential of a cell [28]. Owing to the abundance of arginine found in both CPPs, researchers began developing polyarginines peptides which have become as widely studied as TAT and Penetratin. In polyarginines, sequences greater than 8 amino acids have been shown to be optimal for cellular internalization [28]–[30]. The proposed uptake mechanism is by the formation of a bidentate Hydrogen bond between the negatively charged membrane and the guanidinium group on arginine [28], [29].

The second class, amphipathic peptides, make up the largest class of peptides currently studied today. These CPPs are characterized by their combination of polar (hydrophilic) and non-polar (hydrophobic) regions [28]. Due to the amphiphilic nature of these particles, they tend to from secondary structures in the form of α-helices and β-sheets (β-strands) [28]. This class is made up of three subclasses: primary, secondary, and proline-rich CPPs. Many primary amphiphilic peptides are chimeric in nature, combining a hydrophobic domain, which is essential for cell membrane penetration, to a nuclear localization signal (NLS), often a arginine, lysine, or proline rich motif which deliver cargo to the cell's nucleus through the nuclear pore complex [28]. An example is the Pep-1 sequence, derived from a tryptophan-rich cluster, which is fused to the NLS from the simian virus 40 (SV40) large T antigen (KKKRKV) [31]. Secondary amphiphilic CPPs often take on α-helical structures with hydrophilic and hydrophobic sequences grouped on opposite sides of the helix. An example of this is model amphipathic peptide (MAP), where

Table 1. Cell Penetrating Peptide Sequences

Peptides are divided into three classes, cationic, amphipathic (or amphiphilic) and hydrophobic, based on their amino acid composition. Cationic peptides rely on their overall positive charge to destabilize cellular membranes, while amphiphilic peptides make use of secondary structures resulting from repeating hydrophobic and hydrophilic regions. Hydrophobic peptides make up a small class that are based on hydrophobic chains formed in the peptide. The table below lists several popular peptides, their sequence, number of amino acids sequences and class.

Name	Sequence	AA	Class	Ref
TAT (48-60)	GRKKRRQRRRPPQ	13	Cationic	[23]
Penetratin	RQIKIWFQNRRMKWKK	16	Cationic	[24], [25]
Polyarginine	R_n	n	Cationic	[30]
Pep-1	KETWWETWWTEWSQPKKKRKV	21	Amphipathic	[31]
MAP	KLALKLALKALKAALKLA	18	Amphipathic	[32]
VT5	DPKGDPKGVTVTVTVTVTGKGDPKPD	26	Amphipathic	[33]
PepB3	K $[AAAAEK]_3$ A	20	Amphipathic	[21]
Bac 7 (1-24)	RRIRPRPPRLPRPRPRPLPFPRPG	24	Amphipathic	[34]
C105Y	CSIPPEVKFNKPFVYLI	17	Hydrophobic	[35]

the polar lysine groups align along one side [32]. Additionally, secondary amphiphilic CPPs can form β-sheets (β-strands), such as in VT5 [33]. Finally, proline-rich peptides are unique due to the pyrrolidine ring found in proline, making them unable to stabilize secondary structures. An example is Bac 7, an antimicrobial peptide, which functions as a CPP and an antimicrobial agent [34].

Hydrophobic CPPs are composed from non-polar sequences, which results in their low net charge [28]. This class of CPPs exhibits a high affinity for hydrophobic lipid domains of cells, which is vital to their internalization [28]. This class of CPPs has fewer studies describing their use compared to cationic and amphiphilic, however it has been proposed that they are able to translocate the membrane through an energy-independent method unique from other classes of CPPs [28]. An example of this class is the C105Y peptide, a natural peptide derived from α1-antitrypsin, where its PFVYLI region has been found to act as a NLS [35].

1.3.2. Cell Penetrating Peptide (CPP) Internalization

Currently there are two widely accepted cellular uptake mechanisms: direct penetration and endocytosis (Figure 4). To determine which method is utilized, CPPs can be internalized at either 37 °C (direct penetration and endocytosis) or at 4 °C (direct penetration only) [36]. When cooled to 4 °C, the endocytic ability of the cell is slowed, and any internalization is a result of direct penetration. Direct penetration is a form of energy-independent transduction, which involves an interaction between the positively-charged CPPs and negatively-charged cell membrane, resulting in membrane destabilization. Three direct penetration methods exist: pore formation, carpet, and inverted micelle formation.

Pores exist in two forms, either ‘barrel-stave’ or ‘toroidal’ models. The former creates a cylindrical pore from the peptide which the CPPs can enter through, while in the latter the same pore is formed with a leaflet accumulating on the outer layer. The carpet model describes the accumulation of CPPs on the membrane of a cell, where destabilization occurs as positive charge from the peptides builds up on the negatively charged membrane. Lastly, the inverse micelle mechanism involves the phospholipid bilayer encapsulating peptides on the surface, creating vesicles for transport across the cell membrane which release into the cytosol.

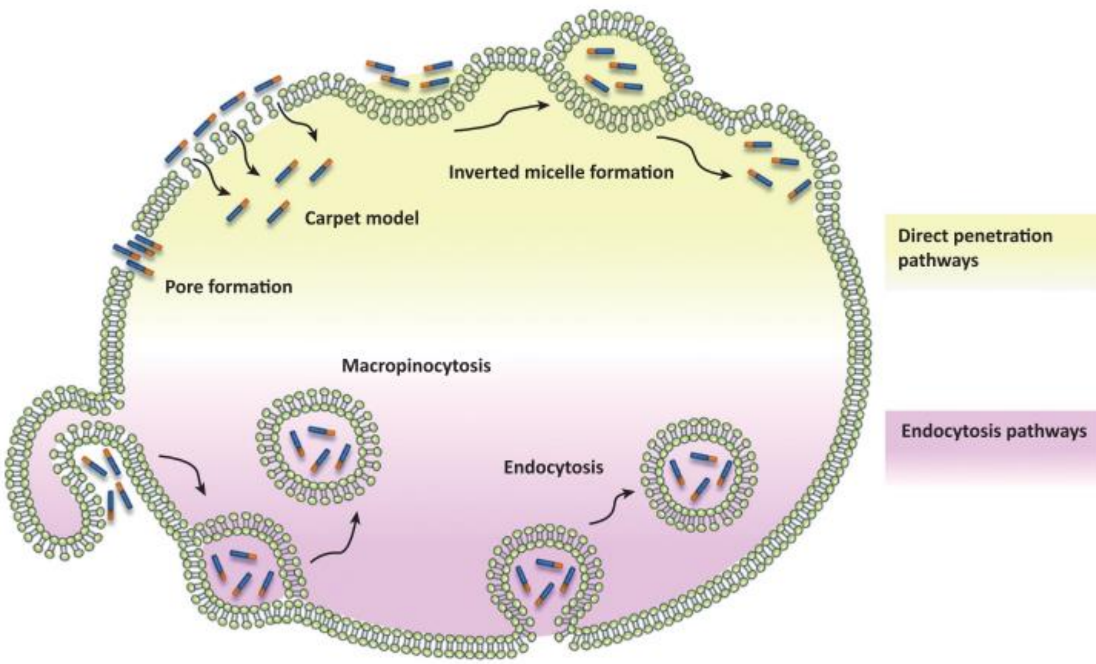

Figure 4. Uptake Mechanisms of Cell Penetrating Peptides (CPPs)

Peptides are internalized by two major pathways, energy independent (Direct penetration) and energy dependent (Endocytosis). Direct penetration is caused by a net positive charge from the CPP which destabilizes the negatively charged membrane. Expression of this pathway includes formation of a peptide-based pore in the membrane, buildup of peptide on the membrane (carpet model) which causes destabilizes and subsequent diffusion, and formation of an inverse micelle by positive charges encapsulation from the membrane. Endocytosis pathways are mediated through some clathrin or caveolin mechanism, and the specific mechanism, macropinocytosis or endocytosis, is based on the size of the peptide being internalized. (Adapted from Guidotti et al. *Trends in Pharma*, 2017)

The second uptake pathway, endocytosis, is an energy-dependent pathway that has been suggested as the principal route for CPPs [37]. There are several different pathways classified as phagocytosis, macropinocytosis, clathrin- or caveolin- mediated endocytosis, and clathrin/caveolin- independent. The determination for which mechanism is utilized is primarily based on the size of the endocytosed molecule. Phagocytosis and macropinocytosis occur through the generation of a pseudopodia which extends out and around the CPP, creating an endosome which facilitates transport into the cytosol. In clathrin and caveolin methods, a pit is formed which the CPP enters and is then coated by either clathrin or caveolin. Independent methods have also been observed by using viral-mediated endocytosis. Regardless of the internalization method, most well-defined peptides have little issue translocating across the membrane. When endocytosis occurs, however, some peptides encounter problems escaping the endosome. Recent studies have shown that the incorporation of an "endosomal escape region" in the form of a hydrophobic amino acid sequence can help facilitate this process [28].

1.3.3. PepB3

One peptide of interest for ATRA delivery is PepB3 (Figure 5). This synthetic peptide is composed of a short repeat sequence (AAAAEK – 6-mer) comprising four alanine (Ala), one glutamic acid (Glu) and one lysine (Lys). This short structure allows the CPP to be modulated in length to tune its size, solubility, and cell penetration capability [21]. This peptide is composed of units containing one positively and negatively charged unit, resulting in a neutral net charge. This peptide is internalized through energy-dependent pathways in the form of an endocytosis. Consistent with other amphiphilic peptides, PepB3 is comprised from a mix of α-helixes and random coils [29]. Previously, this peptide has been used to deliver ATRA and induce differentiation in human neural stem cells [21].

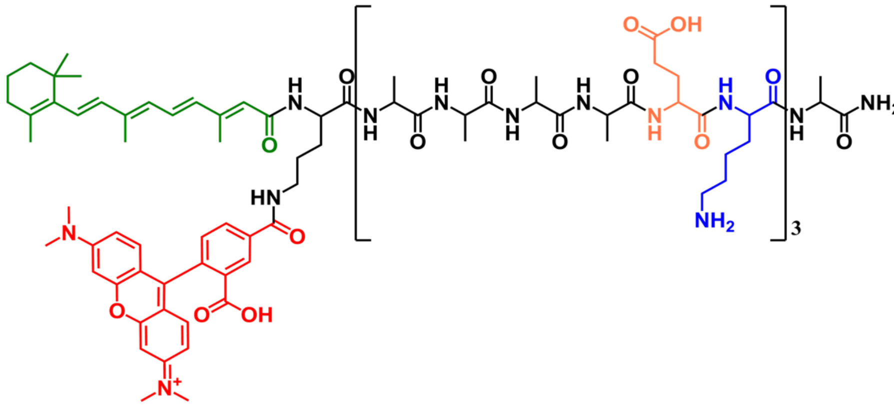

Figure 5. RA-PepB3 Chemical Structure

Chemical structure of RA-PepB3. A PepB unit is composed of four alanine groups (Hydrophobic, Black), a glutamic acid (Orange, Negative) and a lysine (Blue, Positive). This unit can be repeated to enhance secondary structures and delivery efficiency in cell cultures. Conjugated on the peptide is the bioactive drug all-*trans* retinoic acid (Green) and the fluorophore TAMRA (Red) for imaging. (Adapted from Ma et al. Biomolecules, 2016)

1.4. Model Human Neuroblastoma Cell Line, SH-SY5Y

SH-SY5Y cells make an ideal model cell line for differentiation of neuroblastomas. The SH-SY5Y cell line is derived from its parental line, SK-N-SH, which was subcloned three times; first into SH-SY, then SH-SY5, and finally SH-SY5Y. The original SK-N-SH cell line is a neuroblastoma taken in 1970 from a bone marrow biopsy of a 4-year old girl [38]. Being that SH-SY5Y are human-derived cells, they express human specific proteins and protein isomers that would not be found in neural rodent models, such as PC12. Upon differentiation, the cells change from a neuroblast-like state into mature nerve tissue cells, which can be achieved through several methods. Differentiation brings on several new

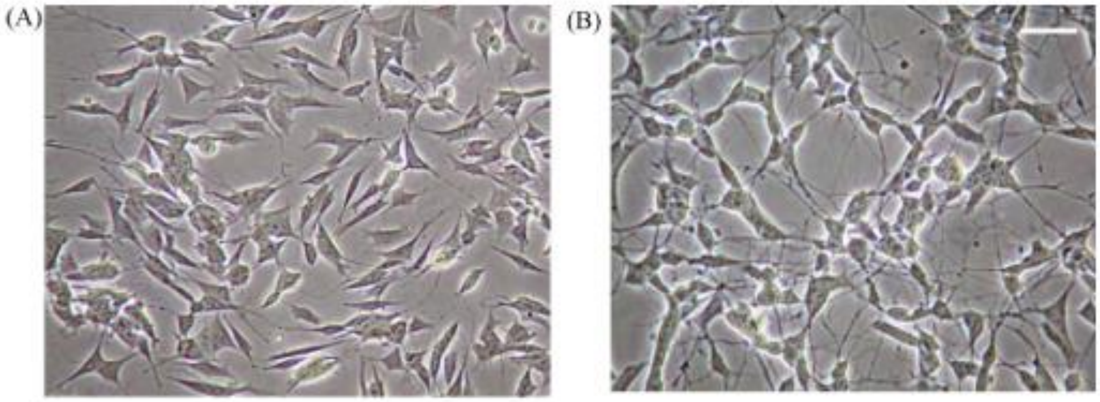

Figure 6. SH-SY5Y Cells

SH-SY5Y cells are a human neuroblastoma cell line derived from bone marrow cells that are commonly used to model differentiation of immature nerve tissue cells. Cells typically spread and exhibit minimal neurite extension under normal proliferation (A), and following treatment with retinoic acid differentiate and extend neurotic processes (B) (Adapted from Cheung et al. *NeuroToxicology* 2009)

characteristics, including formation and extension of neurotic processes and functional synapses, increased electrical excitability of the plasma membrane, and induction of neuron-specific enzymes, neurotransmitters, and neurotransmitter receptors [11].

Undifferentiated SH-SY5Y cells proliferate rapidly and resemble epithelial cells, classified as S-type (surface adherent, Figure 6A) [39]. In culture these cells are mostly adherent and lack many of the neuronal markers found in mature cells [11]. After differentiation, cells decrease proliferation as they transition into mature nerve tissue cells, classified N-type, and begin to extend out branched neurite processes (Figure 6B) [39]. A variety of markers for differentiation can be used, including growth associated protein 43 (GAP43), neuronal nuclei (NeuN), synaptophysin, neuron specific enolase (NSE), microtubule-associated protein-2 (MAP2), and synaptic associated protein-97 (SAP97), while a lack of expression can be found in glial fibrillary acidic protein (GFAP) [11], [39]. There are several methods currently used for differentiation of SH-SY5Y cells, including retinoic acid, phorbol esters, dibutyryl cyclic AMP (dbcAMP), hormones, and brain-derived neurotrophic factor (BDNF) [11], [39]. The most common and best characterized of these methods is retinoic acid. Specific to SH-SY5Y, treatment with retinoic acid promotes survival of the cells through activation of phosphatidylinositol 3-kinase (PI3K)/Akt pathway and upregulation of Bsl-2 protein [11].

2. SPECIFIC AIMS

This thesis seeks to address current problems surrounding all-*trans* retinoic acid (herein abbreviated RA) use in the differentiation of nerve tissue cancer cells by employing the synthetic cell penetrating peptide PepB3 as a vehicle for delivery. Utilizing PepB3's amphipathic structure, it will be incorporated with a retinoic acid group to facilitate transport across the cellular membrane. The peptide will be synthesized, purified, and characterized herein for RA delivery. SH-SY5Y neuroblastoma cells will be treated by theses peptides to quantify and understand their peptides effect, specifically on cytotoxicity, uptake, and differentiation potential. This process will evaluate PepB3's ability as a delivery vehicle compared to the traditional methods of RA differentiation.

Aim 1 – Synthesis and characterization of PepB3 structures

(1.1) Create CPP sequences through solid phase peptide synthesis (SPPS)

(1.2) Purify and isolate by high-performance liquid coronarography (HPLC)

(1.3) Characterize peptides using mass spectrometry (MS)

(1.4) Observe peptide structures by Transmission Electron Microscopy (TEM)

Aim 2 – Characterization of SH-SY5Y differentiation using RA and RA-PepB3

(2.1) Asses toxicity of CPP-mediated retinoic acid delivery on SH-SY5Y cells

(2.2) Monitor CPP uptake using fluorescence microscopy

(2.3) Quantitatively analyze differentiation by neurite length analysis

(2.4) Image SH-SY5Y differentiation using immunocytochemistry

Rationale

While other research has utilized biomaterial delivery mechanisms to facilitate RA transport by mechanisms such as nanoparticles, microspheres, or liposomes, the work of this thesis is the first to do so by incorporating CPPs. CPPs, specifically PepB3 [21], has been shown as a potent vehicle for RA delivery, which is large and rapidly growing field of research with use as a potential cancer treatments. The aims outline a method to create, characterize, and measure CPPs and their effect on cell viability and potential to induce differentiation comparable to current clinical applications utilizing retinoic acid.

3. METHODOLOGY

3.1. Specific Aim 1

For delivery of retinoic acid, PepB3 will be the principal peptide sequence. PepB3 has been shown to be capable of RA delivery in stem cell models [21]. The peptides will be synthesized through solid phase peptide synthesis and tagged with 5-Carboxytetramethylrhodamine (TAMRA), a rhodamine-based fluorescent dye, for monitoring after cellular internalization. Resultant peptides are washed, purified, and isolated with a series of runs through a HPLC. Following isolation, peptide solutions are characterized by weight through mass. Following successful peptide synthesis and characterization, PepB3 will be used *in vitro* to deliver RA to SH-SY5Y.

3.1.1. Peptide Synthesis

Peptide sequences are synthesized through Fluorenylmethyloxycarbonyl chloride (Fmoc) solid phase peptide addition (SPPS) as described previously [21]. Synthesis is performed in a 50 mL reaction vessel on a wrist-action shaker. All steps are performed at room temperature, shaking at 400 RPM. The major steps included (1) swelling, (2) deprotection, (3) conjugation, and (4) cleavage.

(1) Rink Amide resin is swollen in dichloromethane (DCM) for 30 min. The solution is washed three times with dimethylformamide (DMF) for five minutes each.

(2) The Fmoc group is deprotected from the chemical by using a solution of 2% (v/v) 1,8-diazabicyclo[5.4.0]undec-7-ene (DBU) and 2% (v/v) 4-methylpiperidine in DMF. The vessel is given this solution three times for 20 minutes each, totaling 1 hour. The solution is washed three times with DMF for five minutes each.

(3) Amino acids are added sequentially from C to N terminus. Amino acids solutions consist of 6 equivalents of N,N-diisopropylethylamine (DIPEA) and 3 equivalents of hydroxybenzotriazole (HOBt), 2-(1H-benzotriazol-1-yl)-1,1,3,3-tetramethyluronium hexafluorophosphate (HBTU), and the amino acids being conjugated dissolved in DMF. This solution is mixed into the

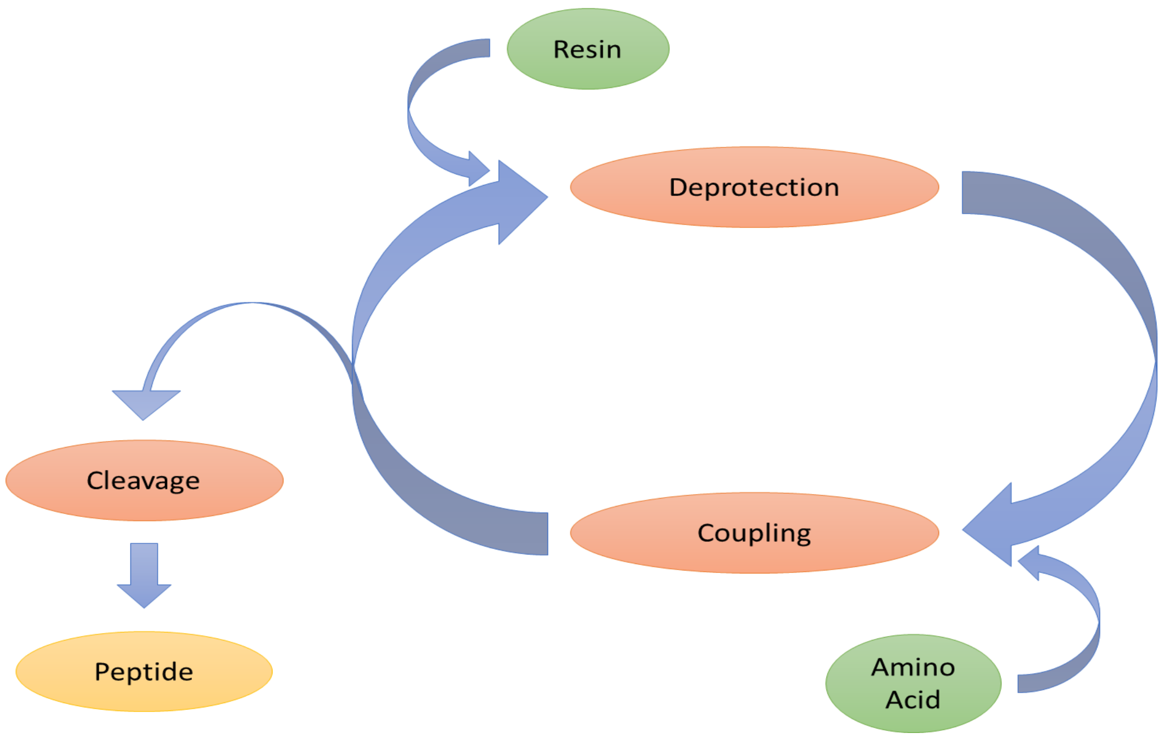

Figure 7. Solid Phase Peptide Synthesis

Resins are used as a base which a peptide is built on. A protecting group is removed from the solution, freeing an amine group for conjugation. Amino acid groups are coupled to the solution C to N terminus, and this cycle of deprotection and coupling is repeated until the peptide is fully synthesized. Following completion, the peptide is cleaved from the resin.

reaction vessel and left to couple overnight. The solution is washed three times with DMF for five minutes each. Steps 2 & 3 were repeated until the peptide was complete.

(3.5) A final deprotection of 1-(4,4-dimethyl-2,6-dioxocyclohex-1-ylidene)-3-ethyl (Dde) groups is done using 2% (v/v) hydrazine in DMF, followed by DMF washing and conjugation of 5(6)-Carboxytetramethylrhodamine (TAMRA).

(4) The solution is washed three times with DMF for five minutes each, followed by three ethanol (EtOH) washes. When the solution is dry, peptides are cleaved from the resin using a solution of 2.5% (v/v) triisopropylsilane (TIPS) and 2.5% (v/v) ultrapure water in trifluoroacetic acid (TFA) for 1 hour.

3.1.2. Peptide Purification & Isolation

Cleaved peptides are air-dried overnight to remove any remaining TFA. Peptides are washed with ice cold diethyl ether through ultrasonication at 4 °C for 30 min. The peptide solution is then centrifuged at 7000 G for 15 min at 4 °C to pelletize. The supernatant is removed, and this process is repeated two more times. The resultant peptide is air-dried overnight to remove remaining ether. The peptides are resuspended in 0.1% (v/v) TFA in water and ultrasonicated until solubilized. This solution is filtered through a 0.22 μm membrane and separated through a reverse HPLC using 0.1% (v/v) TFA in water and 0.1% (v/v) TFA in acetonitrile mobile phases. Collected peptide solution is air-dried to remove TFA, resolubilized in distilled water and lyophilized.

3.1.3. Mass Spectrometry

A small amount of peptide sample was dissolved in 50/50 water/acetonitrile with 0.1% TFA. Samples were injected into a LC/MS/MS system utilizing a C8 stationary column and 0.1% formic acid water/acetonitrile mobile phase. Samples were detected by an ESI-MS system courtesy of Fox Chase Cancer Center (FCCC). Mass spectrum were collected, and peaks were detected by MassLynx. Readings (m/z) were recorded at one fourth and one third of each peptide's exact mass (M/4 & M./4).

3.1.4. Transmission Electron Microscopy

Characterized peptide samples were dissolved in deionized water to a concentration of 10 µM. Samples were loaded onto the carbon side of a TEM grid and prepared using a negative staining protocol. 2 µL of peptide was applied and allowed to air dry for 30 minutes. This process was repeated three times. When dry, 0.1% *w/v* phosphotungstic acid (pH 7.4) was applied to the grid for 15 sec and blotted dry with filter paper. Grids were dried under vacuum for 12 hours. Samples were loaded and imaged on a JEOL JEM 1400 TEM equipped with a Gatan UltraScan 1000 CCD camera.

3.2. Specific Aim 2

SH-SY5Y cells are grown in culture with a proliferation media, and as undifferentiated cells they continue to proliferate indefinitely. To measure the effects of CPP transport of RA, cells will be treated with the following: media, Ac-PepB3, RA-PepB3, and RA. In published research, the standard treatment of cells with RA is 10 µM [11], [39]. CPPs will be delivered across a range of concentrations from 0-10 µM to determine a concentration that is optimal for delivery. Induced cytotoxicity from treatment will be accessed during cell differentiation and differentiation is measured both quantitatively and qualitatively by neurite length analysis and through various imaging techniques, respectively. These combined results will indicate the level to which SH-SY5Y undergoes differentiation following RA treatment via alternative mechanisms.

3.2.1. Cell Culture

SH-SY5Y human neuroblast cells are cultured for biological experiments under standard incubation conditions (37 °C, 5% CO_2). Cells are grown in tissue culture flasks using DMEM media supplemented with 10% (v/v) fetal bovine serum (FBS) and 1% (v/v) pen-strep (PS). This formulation is abbreviated D10FPS. Media is refreshed every 48-72 hours during proliferation. Upon reaching 70% confluency, cells are passaged by removal of media, treated with trypsin and incubated for 5 minutes. Following cell detachment, D10FPS is added and cells are transferred to a centrifuge tube to pelletize at 200 G for 5 min. These cells are split and transferred to a new flask for culture.

3.2.2. Peptide Solution Quantification

Synthesized peptide solutions are sterilized and quantified before treatment with cells. The peptides are dissolved in deionized (DI) water and filtered through a 0.22 µm membrane for sterilization. Because of aggregations from the filtration process, a standard curve is created to determine the concentration of the sterilized peptides. The peptides are serially diluted with known concentrations prepared from unfiltered powder, and 5 µL is added to a 96-well plate. 45 µL of methanol is added to each well to fully solubilize the peptides. The absorbance of the peptides is taken at 554 nm (650 nm reference) correlating to the TAMRA dye. Absorbance measurements are taken on a Tecan infinite M200 Pro plate reader. After calculation of the concentration, peptides are fully dissolved in D10FPS for cell culture. A stock solution for RA is prepared by dissolving in DMSO and filtering through a 0.22 µm membrane for sterilization.

3.2.3. 24 Hour Cytotoxicity

SH-SY5Y cells (passage <10) are seeded in a 96 well-plate at a density of 10,000 cells per well followed by 24 hours incubation to allow attachment and stabilization. Cells are then treated with either Ac-PepB3 or RA-PepB3 at concentrations ranging from 0-10 µM, with a positive and negative control of 10 µM RA and media, respectively. After 24 hours, the cells are washed with D10FPS and treated with PrestoBlue diluted in media at a 1:10 ratio. After 1-hour incubation the plates fluorescence (560/590 nm excitation/emission) is measured using a Tecan infinite M200 Pro plate reader.

3.2.4. Fluorescence & Live-Cell Microscopy

Fluorescence images were taken 24 hours following treatment to visualize peptide localization within cells. Cells were seeded in 96 well plates at 5,000 cells per well and following 24 hours were treated with media (control), 10 µM AC-PepB3, 10 µM RA-PepB3, and 10 µM RA. Live cell images were taken 24 hours following treatment. Cells were washed with PBS to remove latent PepB3 from the well and refreshed with D10FPS prior to imaging. Images were taken on an Olympus IX-83 microscope with a Hamamatsu Ocra-R2 camera and Chamlide live cell incubator system. Differential interference contrast and fluorescence images were taken at 40x magnification. Micrographs were processed using the Olympus plug-in for ImageJ. DIC and fluorescence channels were separated, background corrected using a gaussian filter, auto-contrasted and re-merged.

3.2.5. Z-Stack Imaging

To verify peptide internalization into cells, high magnification z-stack imaging was taken of SH-SY5Y cells. 20,000 cells were seeded onto coverslips that were placed and cultured in a 12 well plate. Treatments of media (control), 10 µM AC-PepB3, 10 µM RA-PepB3, and 10 µM RA were preformed 24 hours following cell seeding. Cells were fixed 24 hours after treatment and nuclei stained with 10 µg/mL of Hoechst 33258 in PBS for 10 minutes at room temperature. Slides were prepared by mounting coverslips using a glycerol solution and imaged on an Olympus IX83 microscope with a 60x objective. Images were obtained at 0.5 µm z intervals and composed using Olympus cellSens Dimension.

3.2.6. 7 Day Cytotoxicity

SH-SY5Y cells (passage <10) are seeded in a 96 well-plate at a density of 5,000 cells per well. After 24 hours incubation to allow for attachment and a stabilization, plates were treated with Ac-PepB3, RA-PepB3, and RA at 1, 5, and 10 µM each, with media as a negative control. Media changes were performed on days 1, 3, and 5 for ongoing plates. Plates were assigned an endpoint of day 1, 3, 5, or 7, and following cell viability testing were removed. At a plate's endpoint, cells were treated with PrestoBlue diluted in media at a 1:10 ratio. Following 1-hour incubation, the plates fluorescence (560/590 nm excitation/emission) is measured using a Tecan infinite M200 Pro plate reader.

3.2.7. SH-SY5Y Differentiation & Neurite Length Analysis

Differentiation studies are performed for a duration of 7 days. Cells were seeded at a density of 5,000 cells per well followed by 24 hours incubation to allow for attachment and stabilization. Following, media was exchanged and treated with 10 µM of Ac-PepB3, RA-PepB3, and RA. Treatments were refreshed every 48 hours until their endpoint where cells are fixed with 4% paraformaldehyde (PFA) at room temperature for 15 min, followed by washing with PBS.

Images were taken at day 1, 3, 5, and 7 to monitor cell differentiation and neurite outgrowth in response to different treatment groups. Images were taken on an Olympus IX83 microscope with a Hamamatsu camera at 40x magnification. Micrographs were processed in ImageJ by background correcting using a gaussian filter and auto-contrasting images. Neurites were measured in ImageJ by using the freehand draw tool to manually measure individual neurite lengths. Neurites at least twice the length of the cell body were measured (Figure 8).

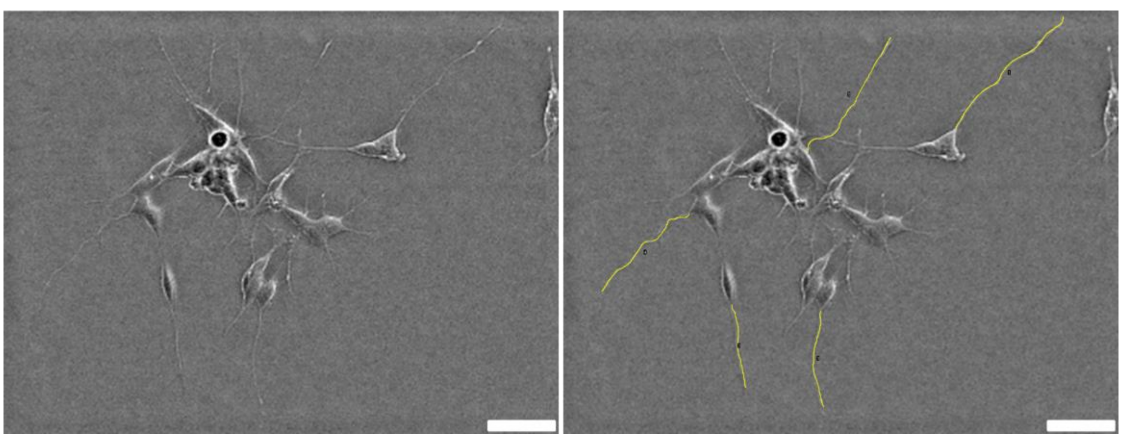

Figure 8. Neurite Length Analysis Methodology

Example image representing neurite sizing methodology. Images were measured for each condition using the ImageJ freehand tool to trace neurites. Measurements begins at the point where the neurite protrudes from the cell body outward towards each neurite's endpoint. Yellow lines show representative neurite length measurements. Scale Bar = 50 µm.

3.2.8. Immunocytochemistry (ICC)

Cells were fixed with 4% PFA at room temperature for 10 minutes and rinsed with PBS. After rinsing, cells were blocked and permeabilized simultaneously in a buffer of 5% donkey serum, 0.3% Triton-X, and 0.02% sodium azide for 30 minutes at room temperature. Primary antibodies (Rb x GAP43) were diluted in the blocking buffer at 1:200 and applied for 16-24 hours at 4 °C. Secondary antibodies (Dky x Rb FITC) were diluted in the blocking buffer at 1:200 for 1 hour at room temperature. Nuclei were counterstained with 10 µg/mL Hoechst 33258 in PBS for 10 minutes at room temperature and cells were imaged on an Olympus IX-83 microscope with a Hamamatsu Ocra-R2 camera. Images were processed using the Olympus plug-in for ImageJ by separating channels, auto-contrasting, and re-merging pictures.

3.2.9. Corrected Total Cell Fluorescence (CTCF)

ICC images were quantified by measurement of corrected total cell fluorescence (CTCF) using a previously described method [40]. Briefly, in ImageJ, the area of a cell is outlined using its and the integrated density of the fluorescent channel is calculated. This function takes a greyscale image of the cell, determines it's mean grey area and is multiplied by the cell's area, giving the total cell fluorescence. The background is determined by measuring the mean grey are of a small area adjacent the cell and multiplying by the area of the cell. The CTCF is determined by subtracting the background value from the total cell fluorescence.

3.2.10. Neuron Polarity

Neuronal polarity was assayed on cells differentiated for 7 days, with measurements were taken on days 1, 3, 5, and 7. Processes originated from the cell body were counted as single neurons. Images were taken on an Olympus IX83 microscope with a Hamamatsu camera at 40x magnification.

3.2.11. Long Term Cytotoxicity & Differentiation

SH-SY5Y cells (passage <10) are seeded in a 96 well-plate at a density of 5,000 cells per well. After 24 hours, plates were treated with Ac-PepB3, RA-PepB3, and RA at 10 µM each, with media as a negative control. Media changes were performed every 48 hours. Plates were assigned an endpoint of day 10, 12, or 14 and following cell viability testing were removed. At a plate's endpoint, cells were treated with PrestoBlue diluted in media at a 1:10 ratio. Following 1-hour incubation, the plates fluorescence (560/590 nm excitation/emission) is measured using a Tecan infinite M200 Pro plate reader.

3.2.12. Statistical Analysis

Statistical significance of experiments is determined using JMP Pro 14, with all results expressed as mean ± S.E.M. Quantitative data is analyzed using a one-way analysis of variance (ANOVA) followed by a Tukey HSD test to determine individual group significance. Significance is reported as * ($p<0.05$), ** ($p<0.01$), or *** ($p<0.001$).

4. RESULTS

4.1. Aim 1

4.1.1. Mass Spectrometry

Peptide synthesis was verified through mass spectrometry. The instrument used to determine the mass of the synthesized peptides has a detection limit of 2,000 m/z, below the actual mass of the synthesized peptides (approximately 2,300-2,500). As a sample travels through the instrument, it becomes positively charged and energetically unstable. As the positive ions continue to accelerate through the instrument, they get detected by the mass spectrometer. PepB3 peptides contain primary amine groups on each of the three lysine groups as well as the N-terminus provides four sites that become protonated. The instrument measures a molecules m/z, or mass per charge. Since PepB3 has four available positive ion sites, the detected mass will appear as one fourth its actual mass, or M/4. Some molecules do not fully protonate, leading to detection of a lesser number of M/3 molecules. The mass spectrometry results for the synthesized peptides are outlined in Table 2, and the mass spectrums are shown in Figure 9-10.

Table 2. Mass Analysis of Peptide Sequences from MS

Samples are positively charged as they travel through the mass spectrometer and are protonated at the open amine groups on the three repeated lysine groups and the C-terminus. Results are displayed as m/z, or mass per charge. Detected readings were measured at one fourth and one third the mass of the peptide. ESI-ToF: electrospray ionization time-of-flight.

Name	Actual Mass (Da)	ESI-Tof Measured Mass – M/4 (m/z)	ESI-Tof Measured Mass – M/3 (m/z)
RA-PepB3	2,535.36	635.73	847.66
Ac-PepB3	2,295.18	574.65	765.91

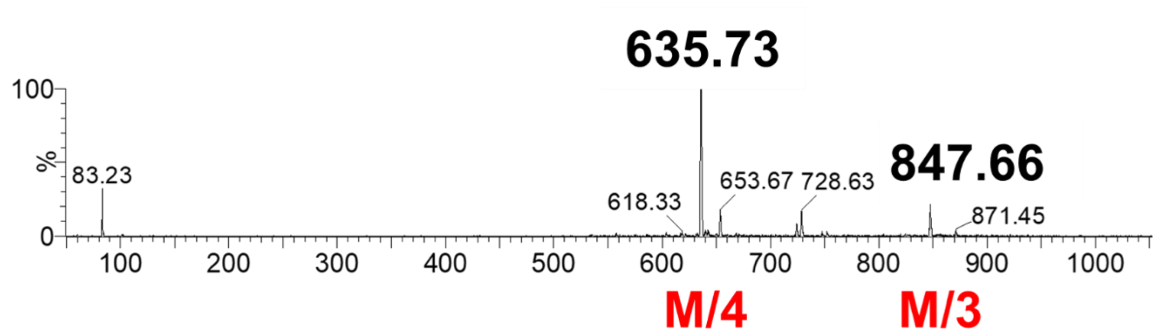

Figure 9. RA-PepB3 Mass Spectrometry Results

RA-PepB3 ($C_{123}H_{184}N_{27}O_{31}^{+}$) has a molecular weight of 2,536.98 g/mol and an exact mass of 2,535.36 Da. Sample was measured using an ESI-MS at FCCC. Detected peaks at M/4 and M/3 are highlighted

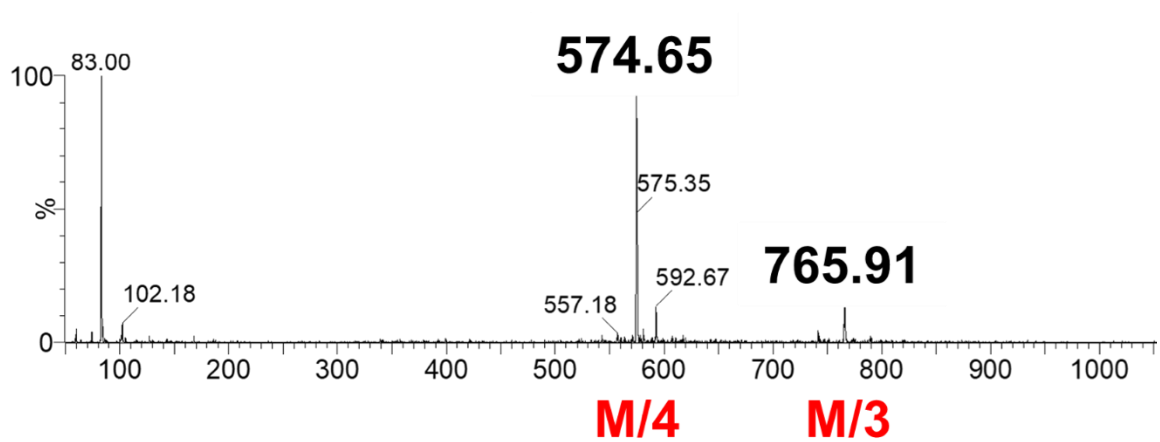

Figure 10. Ac-PepB3 Mass Spectrometry Results

Ac-PepB3 ($C_{105}H_{160}N_{27}O_{31}^{+}$) has a molecular weight of 2,296.59 g/mol and an exact mass of 2,295.18 Da. Sample was measured using an ESI-MS at FCCC. Detected mass peaks at M/4 and M/3 are highlighted.

4.1.2. Transmission Electron Microscopy

Transmission electron microscopy (TEM) images were obtained of sample to visualize secondary structures. Micrographs show peptides orienting in long strands with a coiled structure (Figure 11).

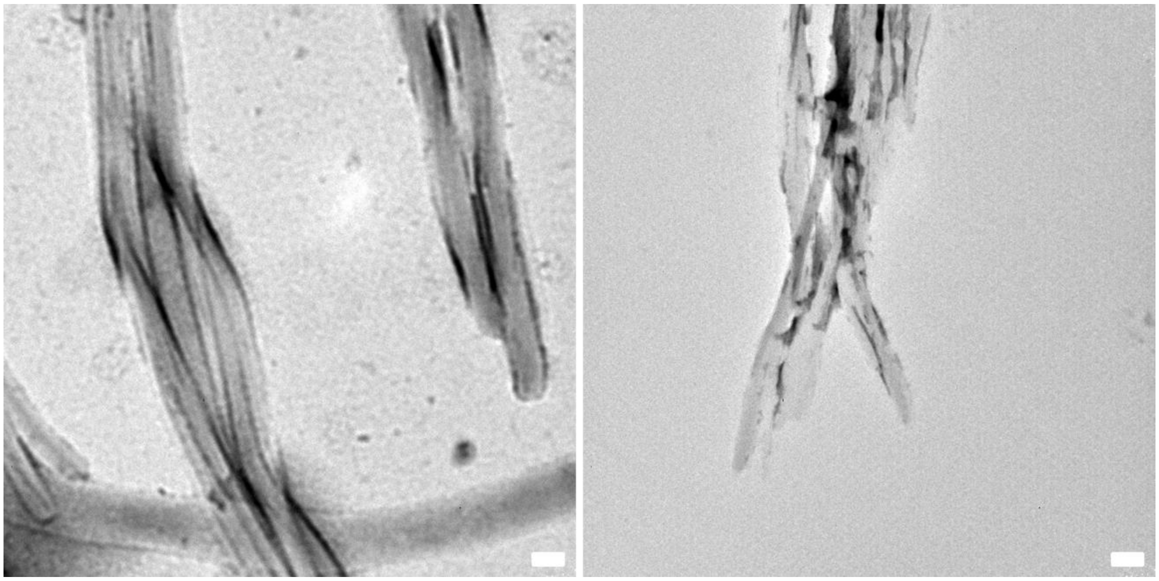

Figure 11. PepB3 TEM Analysis Results

TEM micrographs of Ac-PepB3 (left) and RA-PepB3 (Right). Secondary α-helical structures previously determined can be visualized [21]. Scale Bar = 100 nm

4.2. Aim 2

4.2.1. 24 Hour Cytotoxicity

Prior to long term studies involving the fabricated peptides, a short-term cytotoxicity study was conducted to identify any cytotoxic effects following treatment of SH-SY5Y cells. 96 well-plates were seeded with 10,000 cells/well and treated after 24 hours with PepB3 peptides across a range of concentrations. Selected treatment doses were chosen from 0-10 µM to establish a concentration that could potentially induce differentiation in cells without damage to the cells. A max dose of 10 µM was chosen as a limit based studies which utilize this treatment effectively with RA alone [11], [39]. Included in this trial were two additional treatment groups, media (negative control) and 10 µM RA (positive control). No significant effect was found on cells up to the max dose of 10 µM with either RA-PepB3 or Ac-PepB3 (Figure 12).

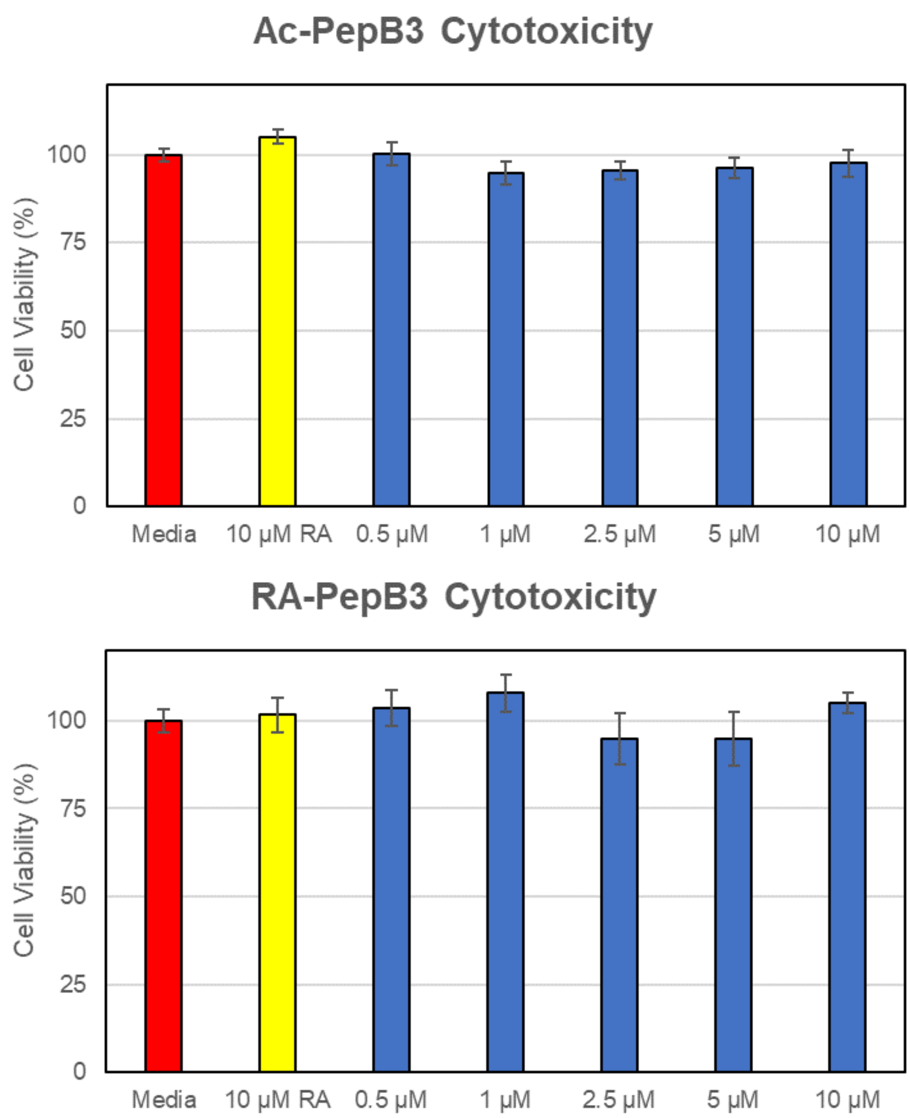

Figure 12. 24 Hour RAPepB3 and Ac-PepB3 Cytotoxicity Results

Cytotoxicity of SH-SY5Y cells after 24 hours treatment with PepB3 structures. Cells were treated with a range of 0-10 µM of Ac-PepB3 or RA-PepB3, and with 10 µM RA. No significant difference was noticed in any of the treatment groups. Values are represented as average ± S.E.M. N=12.

4.2.2. Peptide Uptake

Following 24-hour treatment, peptide localization was observed by red fluorescence emission of TAMRA. Fluorophores conjugated to peptide during synthesis allow for *in-vivo* analysis via fluorescence microscopy. In both positive and negative

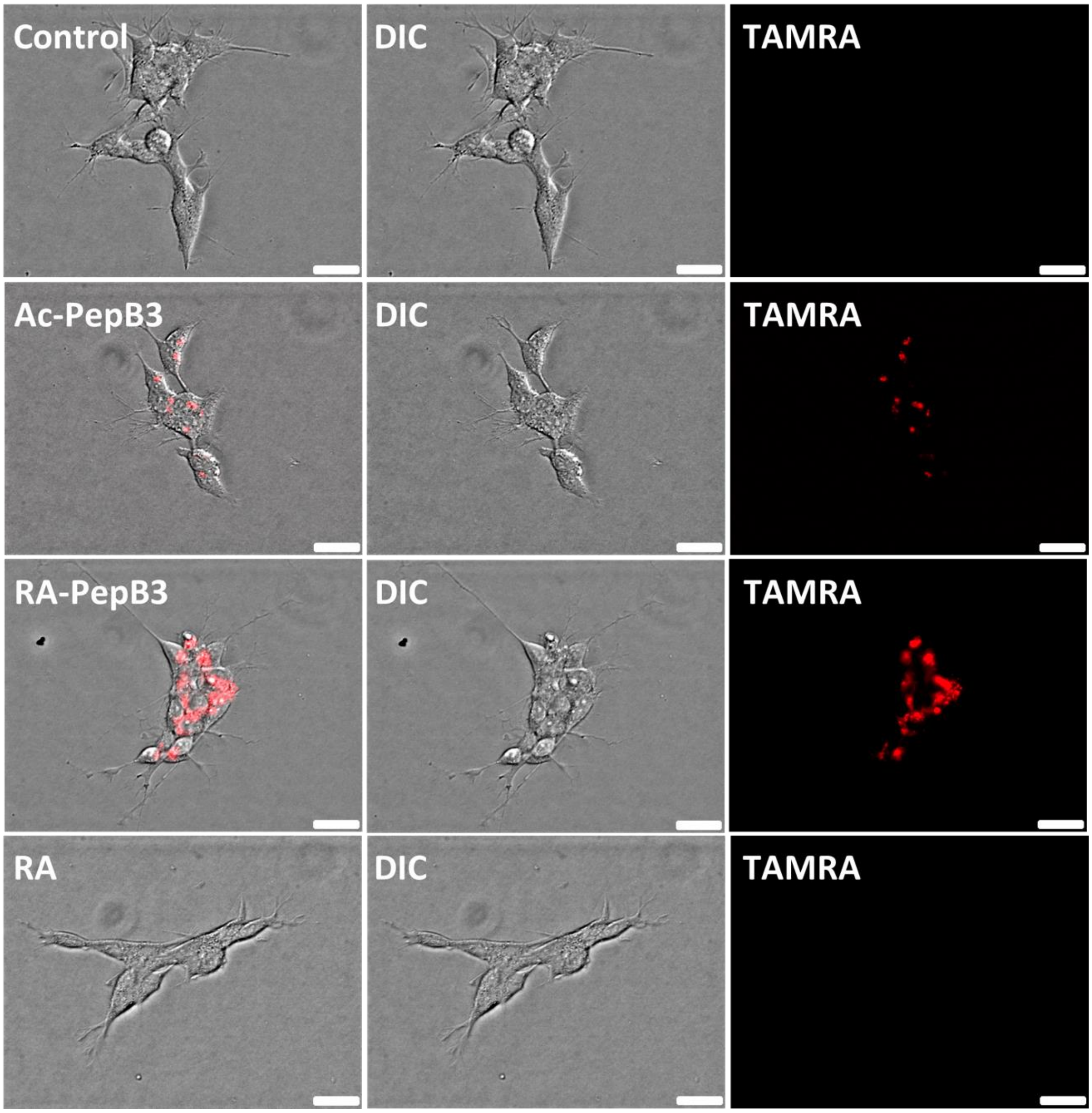

Figure 13. PepB3 Cellular Localization Study Results

Fluorescence images showing peptide localization in SH-SY5Y cells. Red channel signal corresponds with TAMRA fluorophore conjugated to PepB3 structures during synthesis. Cells were imaged 24 hours following treatment. Scale bar = 25 µm.

controls, 10 µM RA and media, no fluorescent signal was detected in the fluorescence micrographs, while both 10 µM Ac-PepB3 and 10 µM RA-PepB3 peptides showed expression of the internalized peptide by TAMRA fluorophore (Figure 13).

4.2.3. Z-Stack Imaging

Z-stack images were taken of SH-SY5Y cells 24 hours following RA-PepB3 treatment. Cells were stained with Hoechst to visualize nuclei, and images taken show PepB3 uptake within the cell body adjacent the nucleus (Figure 14).

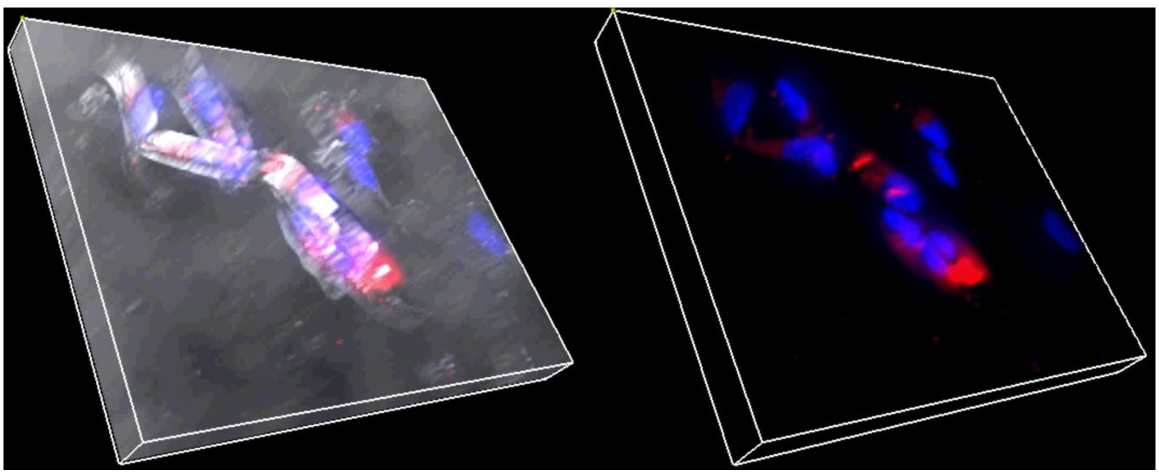

Figure 14. Z-Stack Microscopy Analysis Results

Z-Stack imaging of RA-PepB3 uptake into SH-SY5Y cells. TAMRA (Red, conjugated to RA-PepB3) fluorescence is observed within the cell body. Nuclei are counterstained with Hoechst 33258.

4.2.4. 7 Day Cytotoxicity

Differentiation experiments were planned for a time-period of seven days, and in conjunction with these experiments a secondary cell viability experiment was preformed to monitor toxicity from PepB3 over the course of a week. Prior literature has shown that long exposure to 10 µM retinoic acid can cause cytotoxic effects that are not observed in shorter viability assays [21]. Three concentrations of Ac-PepB3, RA-PepB3 and RA were chosen for this experiment at 1, 5, and 10 µM and cell viability was measured at days 1, 3, 5, and 7 (Figures 15-17).

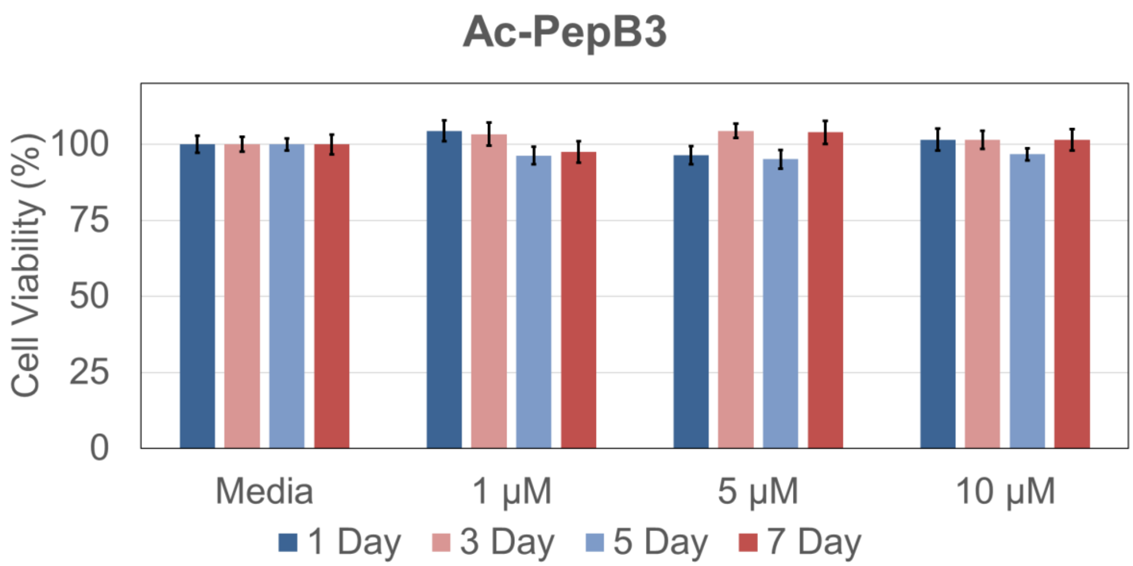

Figure 15. Ac-PepB3 Cell Viability Results

Cytotoxicity of SH-SY5Y cells over 7-day time-period treated 1, 5, and 10 µM Ac-PepB3. Viability was analyzed through ANOVA testing with a Tukey HSD post-hoc. Reported significance relates the value to that day's control(media). Values are represented as average ± S.E.M. N=12.

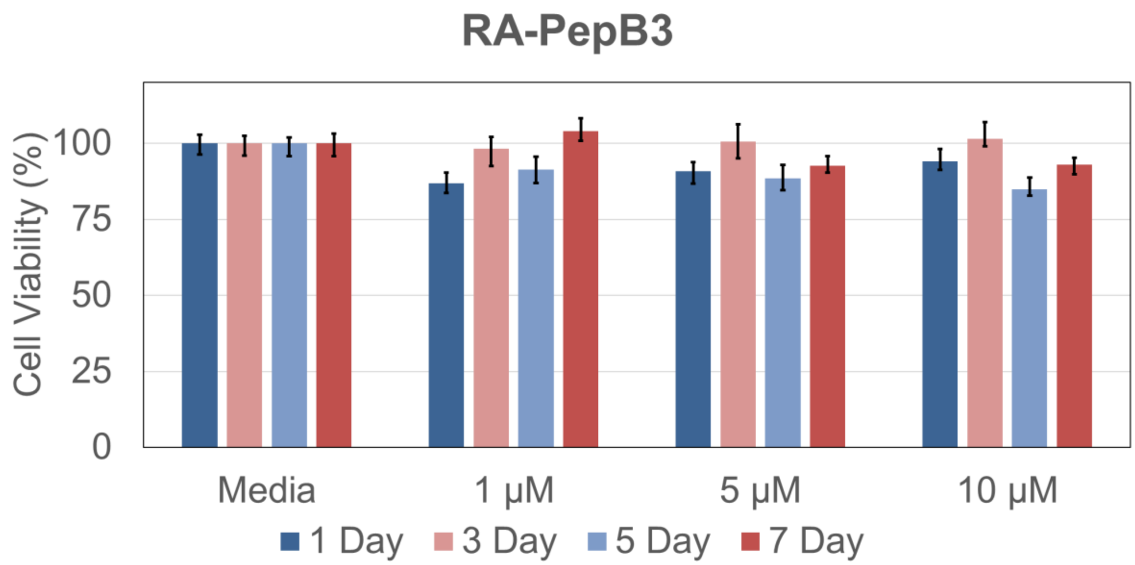

Figure 16. RA-PepB3 Cell Viability Results

Cytotoxicity of SH-SY5Y cells over 7-day time-period treated 1, 5, and 10 μM RA-PepB3. Viability was analyzed through ANOVA testing with a Tukey HSD post-hoc. Reported significance relates the value to that day's control(media). Values are represented as average ± S.E.M. N=12.

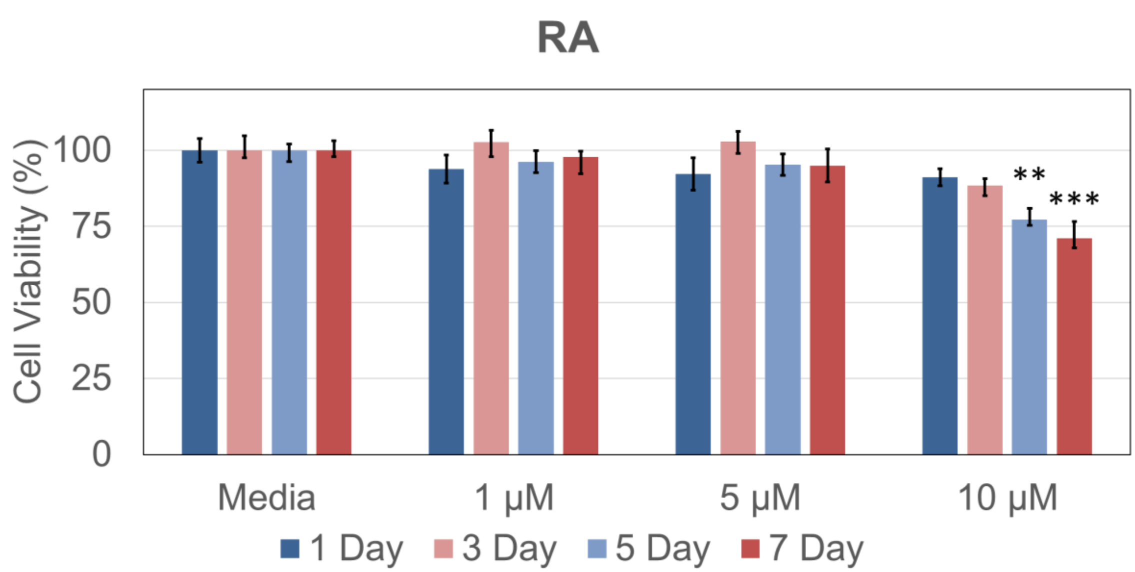

Figure 17. Retinoic Acid Cell Viability Results

Cytotoxicity of SH-SY5Y cells over 7-day time-period treated 1, 5, and 10 μM RA. Viability was analyzed through ANOVA testing with a Tukey HSD post-hoc. Reported significance relates the value to that day's control(media). Values are represented as average ± S.E.M. N=12. Significance is reported as * ($p<0.05$), ** ($p<0.01$), or *** ($p<0.001$).

4.2.5. Neurite Length Analysis

After determining cell viability and peptide internalization, experiments were conducted to measure the differentiation of SH-SY5Y cells when treated with Ac-PepB3, RA-PepB3 and RA (10 µM). The control group received D10FPS throughout the differentiation. Cells were treated 24 hours following seeding, and media changed every 48 hours for 7 days. Differentiation was quantified by measurement of neurite lengths present at timepoints 1, 3, 5, and 7 (Figure 20-23). Quantified lengths show a significant increase in neurite length in both RA-PepB3 and RA, with no significant difference between RA-PepB3/RA and Control/Ac-PepB3 (Figure 18-19).

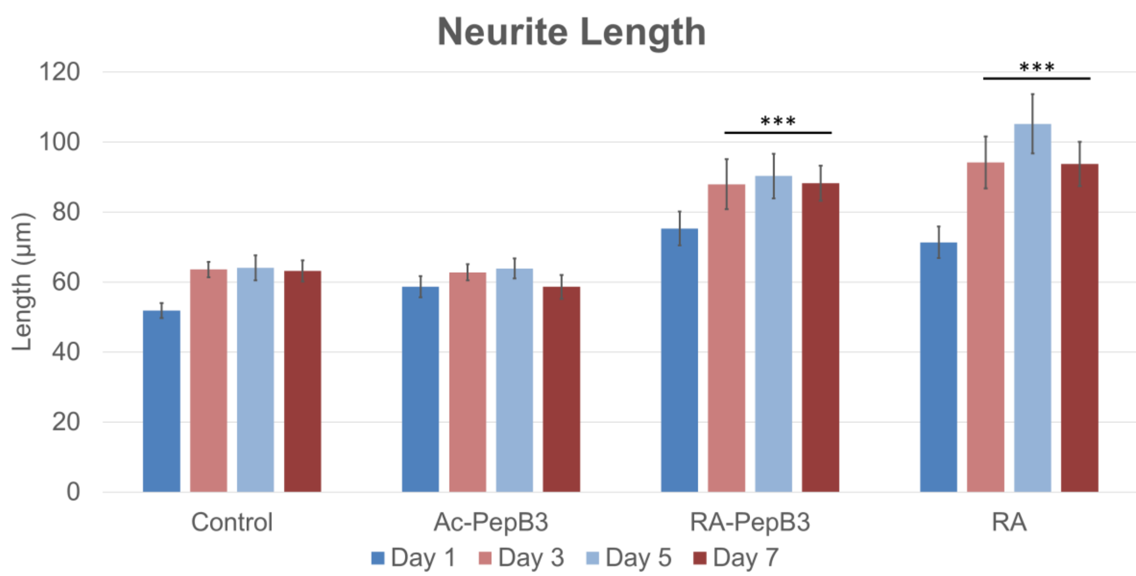

Figure 18. 7 Day Neurite Length Analysis Results

SH-SY5Y cell differentiation progression over a period of 7 days. Cells were treated following 24 hours, and treated when media was refreshed on days 1, 3, and 5. Values are represented as average ± S.E.M. N=30. Significance is reported as * ($p<0.05$), ** ($p<0.01$), or *** ($p<0.001$).

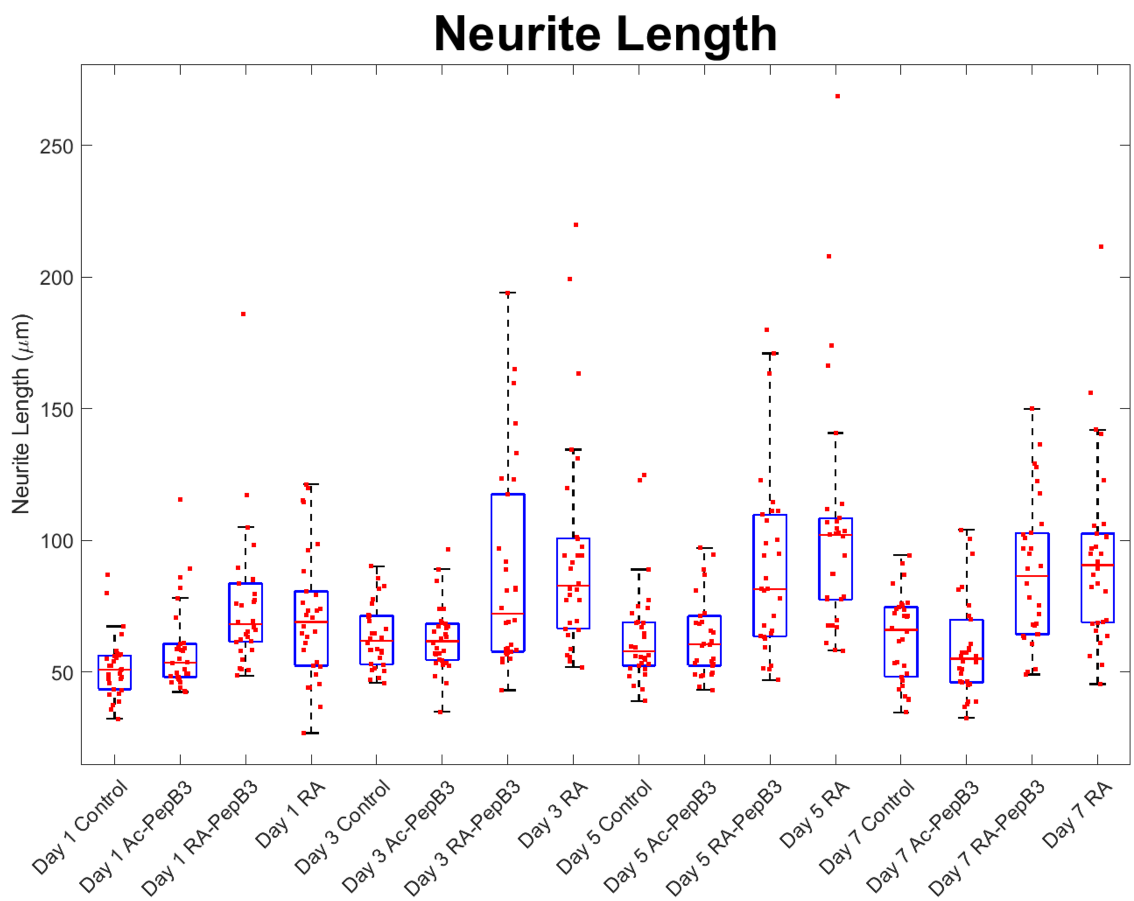

Figure 19. Neurite Length Jitter Plot Results

SH-SY5Y cell differentiation progression over a period of 7 days. Cells were treated following 24 hours, and treated when media was refreshed on days 1, 3, and 5. Values are represented as average ± S.E.M. N=30.

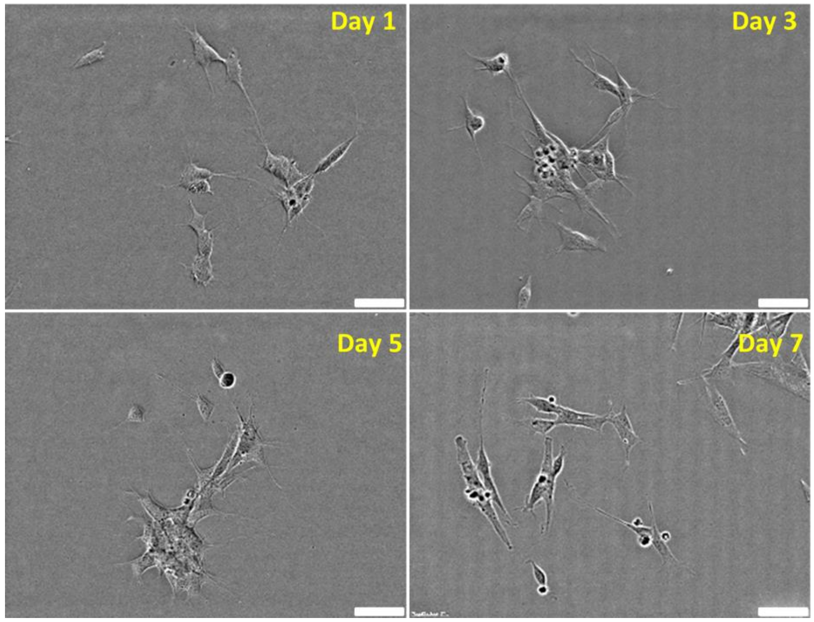

Figure 20. Control (Media) SH-SY5Y Differentiation Results

SH-SY5Y cell differentiation progression over a period of 7 days. Cells were treated following 24 hours and media was refreshed on days 1, 3, and 5. Scale bar=50 µm.

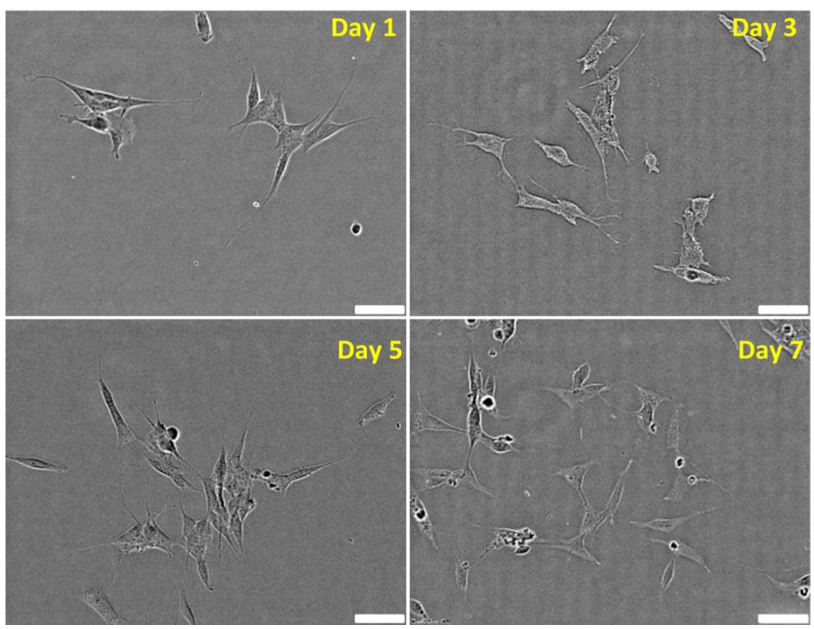

Figure 21. Ac-PepB3 SH-SY5Y Differentiation Results

SH-SY5Y cell differentiation progression over a period of 7 days. Cells were treated following 24 hours and treated with 10 µM Ac-PepB3 when media was refreshed on days 1, 3, and 5. Scale bar=50 µm.

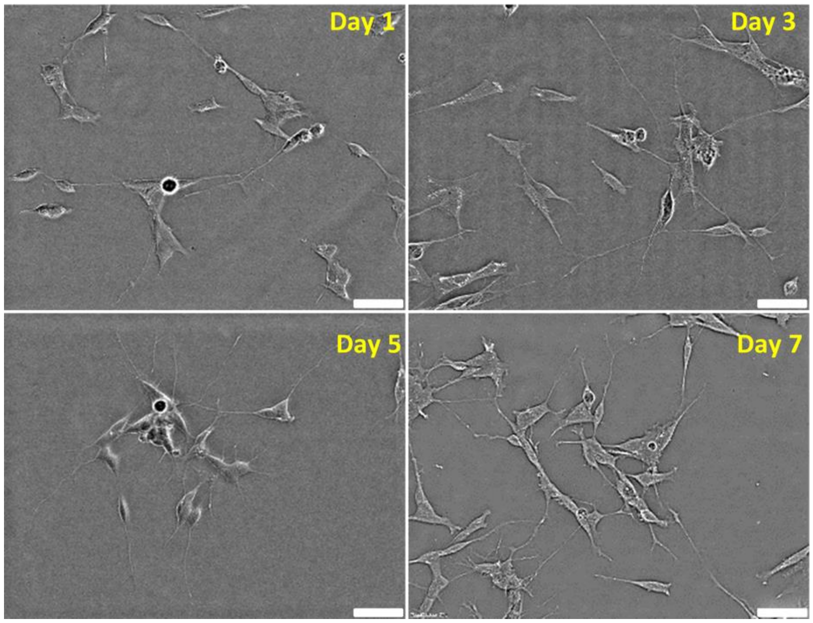

Figure 22. RA-PepB3 SH-SY5Y Differentiation Results

SH-SY5Y cell differentiation progression over a period of 7 days. Cells were treated following 24 hours and treated with 10 µM RA-PepB3 when media was refreshed on days 1, 3, and 5. Scale bar=50 µm.

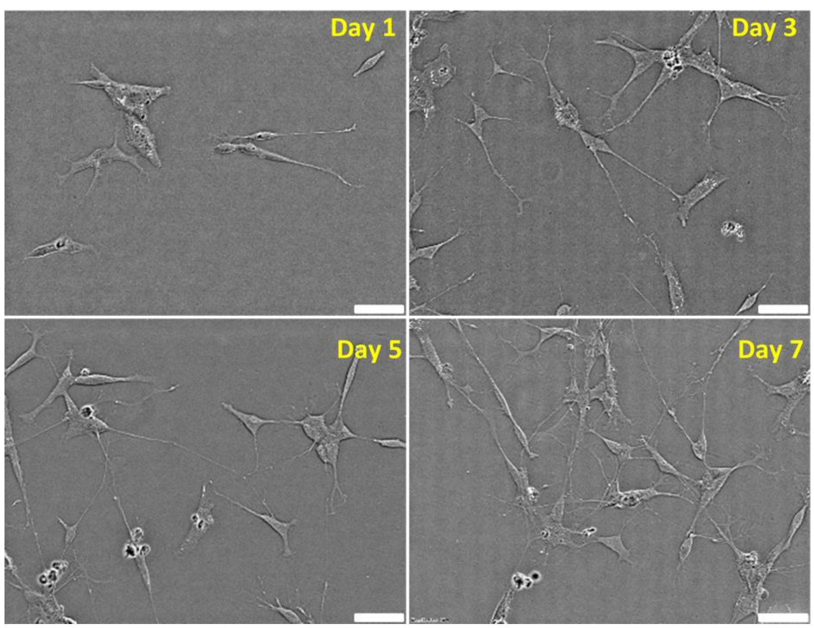

Figure 23. Retinoic Acid SH-SY5Y Differentiation Results

SH-SY5Y cell differentiation progression over a period of 7 days. Cells were treated following 24 hours and treated with 10 µM RA when media was refreshed on days 1, 3, and 5. Scale bar=50 µm.

4.2.6. Immunocytochemistry

Immunocytochemistry (ICC) was performed on cells fixed after 3 and 7 days looking for GAP43 expression. The GAP43 protein is expressed during nerve growth as cells differentiate into neuronal cells. While this is protein is often used as a marker for differentiation in SH-SY5Y cells, [41], it's expression has been shown to decrease after initial neurogenesis (around day 3) and returns to baseline expression. This was observed in our cells where neurons were positively stained at day 3 (Figure 25) with a reduction by day 7 (Figure 26). At day 3, RA-PepB3 and RA cells expressed a 2.5x fold increase in fluorescence intensity compared to control treatments (Figure 24).

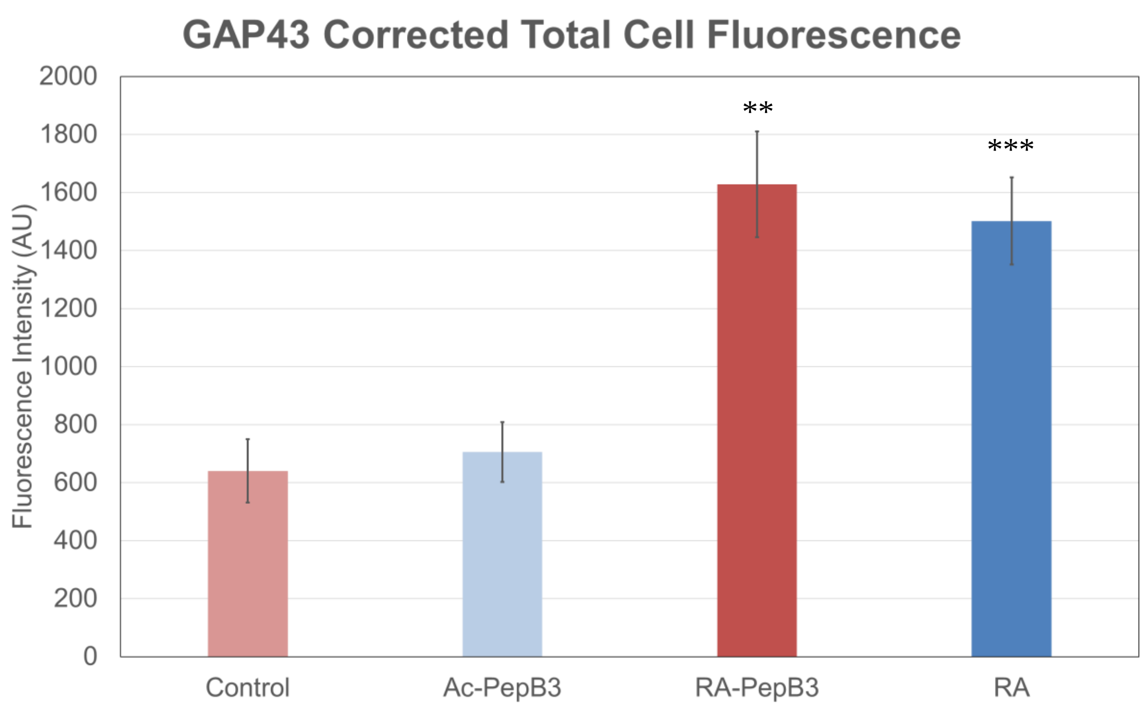

Figure 24. Day 3 GAP 43 Corrected Total Cell Fluorescence (CTCF) Results

Total cell fluorescence of GAP43 expression in SH-SY5Y cells. Expression was measured following three days of differentiation. Values are represented as average ± S.E.M. N=30. Significance is reported as * ($p<0.05$), ** ($p<0.01$), or *** ($p<0.001$).

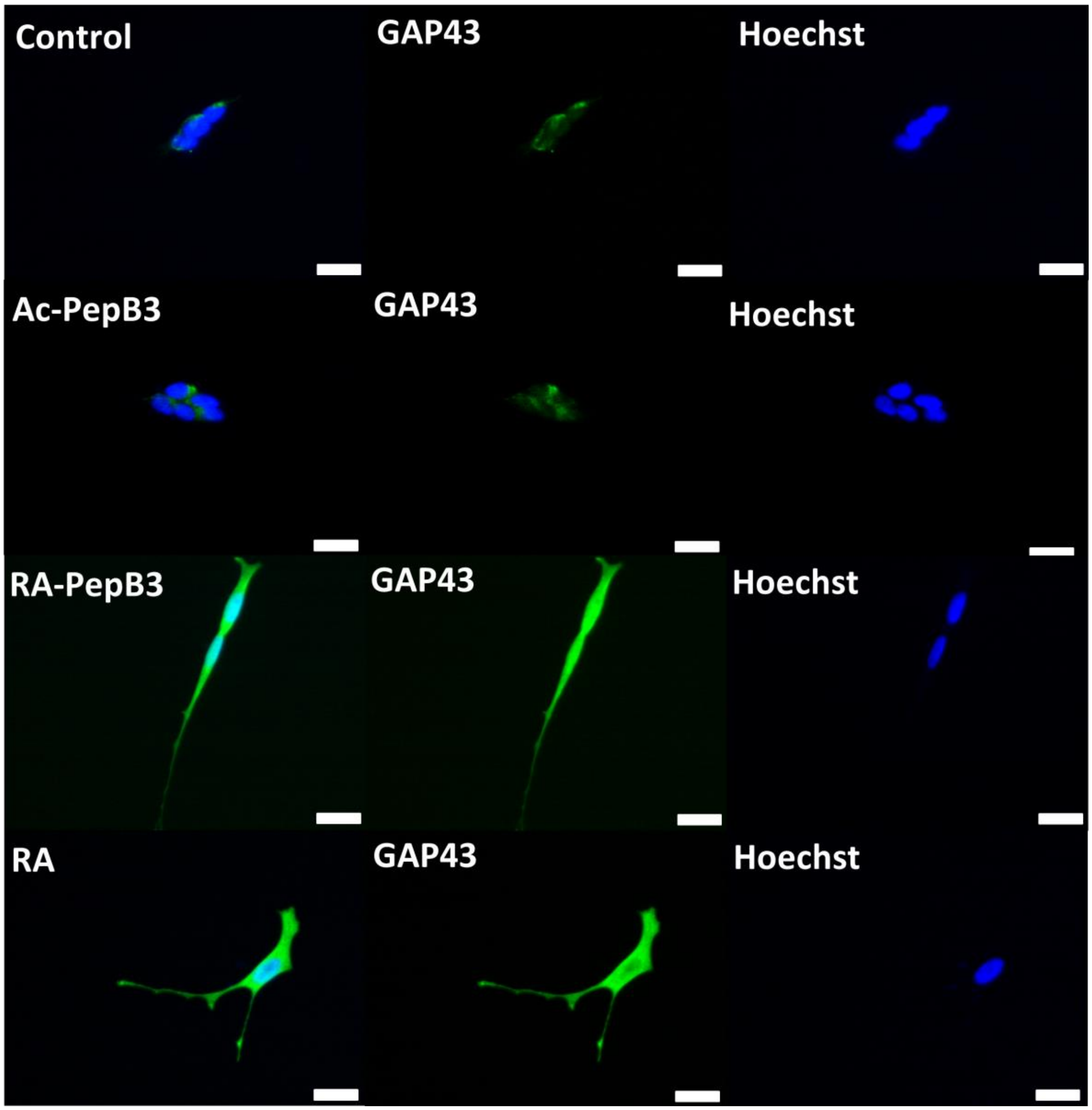

Figure 25. Day 3 GAP43 Expression Results

GAP43 expression following 3 days treatment. GAP43 is a cytoplasmic protein expressed during neurite genesis in cells. Neurogenesis peaks at day 3 in treated cells before returning to baseline expression. Cells were fixed and stained for GAP43 with a nuclear Hoechst 33258 counterstain. Scale bar=50 µm.

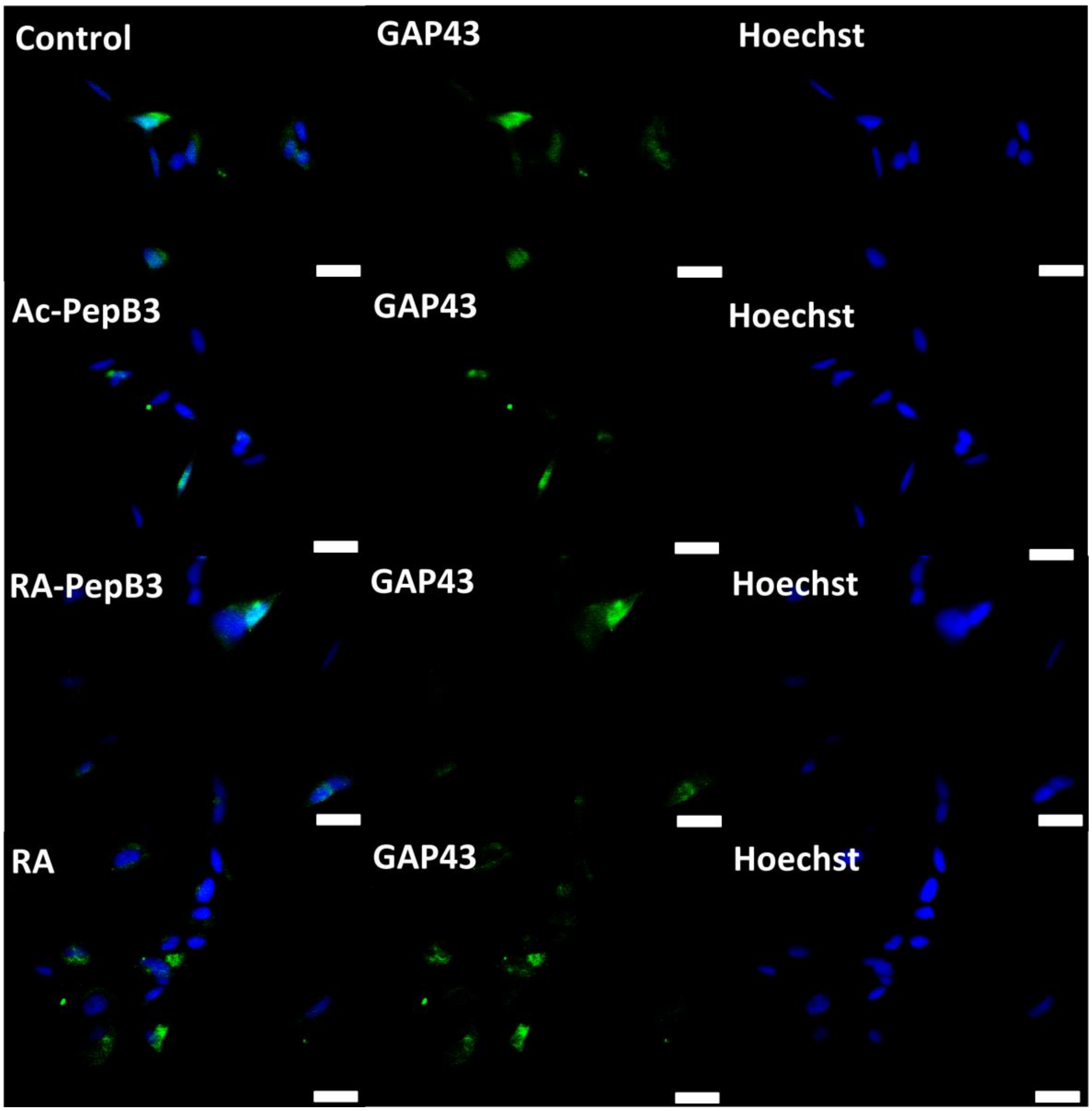

Figure 26. Day 7 GAP43 Expression Results

GAP43 expression following 7 days treatment. GAP43 is a cytoplasmic protein expressed during neurite genesis in cells. Neurogenesis peaks at day 3 in treated cells before returning to baseline expression. Cells were fixed and stained for GAP43 with a nuclear Hoechst 33258 counterstain. Scale bar=50 µm.

4.2.7. Neuron Polarity

Cell polarity was measured by counting of neurite processes originating from the cell body to determine if treatment with RA had a significant effect on cell morphology. No significant difference in cell polarity was observed in and condition (Figure 27).

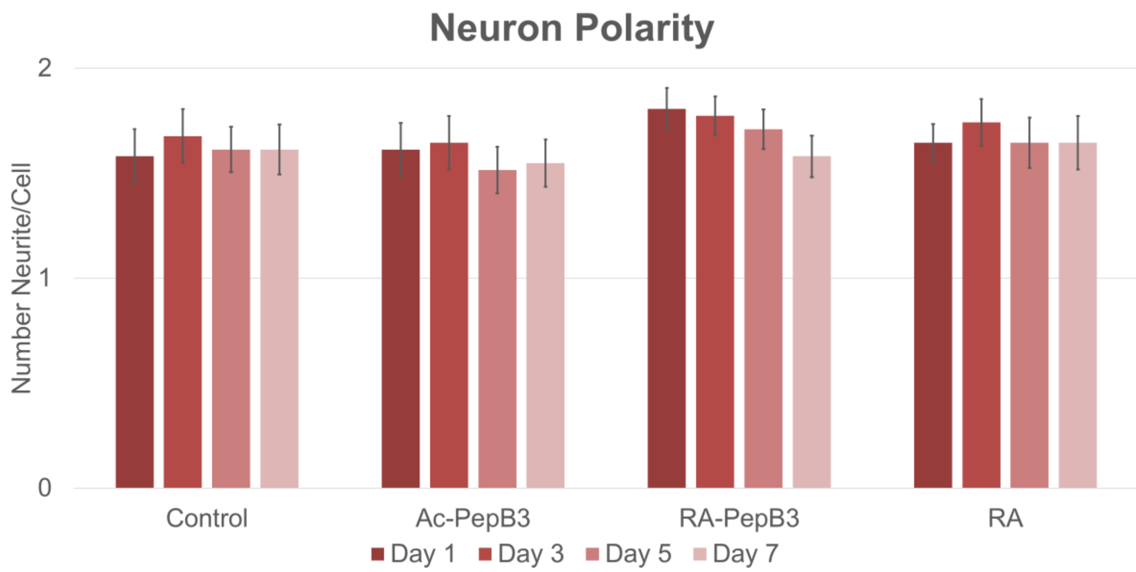

Figure 27. Cell Polarity Quantification Results

To quantify the presence of unipolar, bipolar, and multipolar cells present in SH-SY5Y, the number of neurites per cell. No significant change in polarity was detected in any of the treatment groups. Values are represented as average ± S.E.M. N=30.

4.2.8. Long Term Cytotoxicity & Differentiation

Plates seeded for long term differentiation showed increased effect from retinoic acid toxicity with continued viability in untreated and PepB3 conditions. Viability of RA dropped to 33% by day 14 (Figure 29). At the trial's endpoint, neurite length measurement was ceased due to crowding of the well by rapidly proliferative S-type cells. While N-type cells remain, clear images could not be obtained for all conditions (Figure 28).

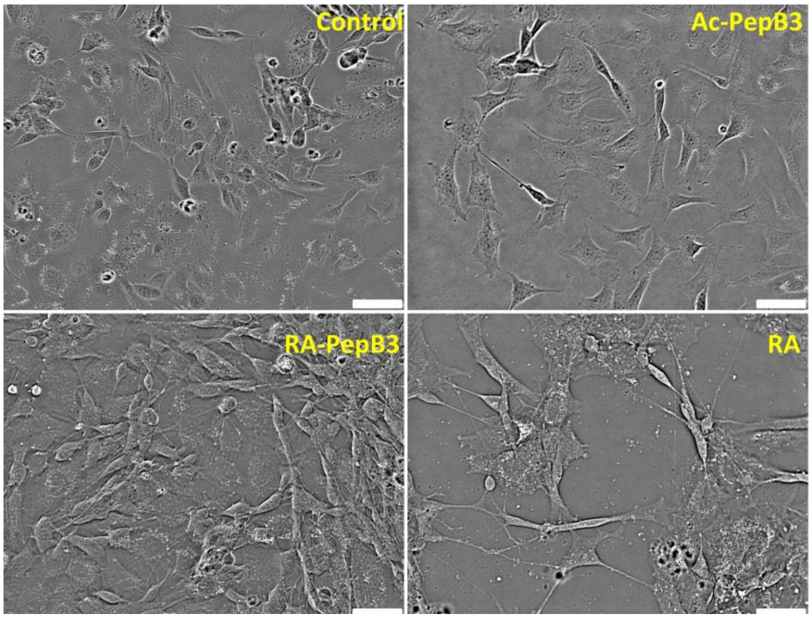

Figure 28. 14 Day Differentiation Results

SH-SY5Y cells following 14 days differentiation. While N-type cells remain present in RA-PepB3 and RA treatments, all conditions exhibit a large increase to S-type proliferation. Scale bar = 50 µm.

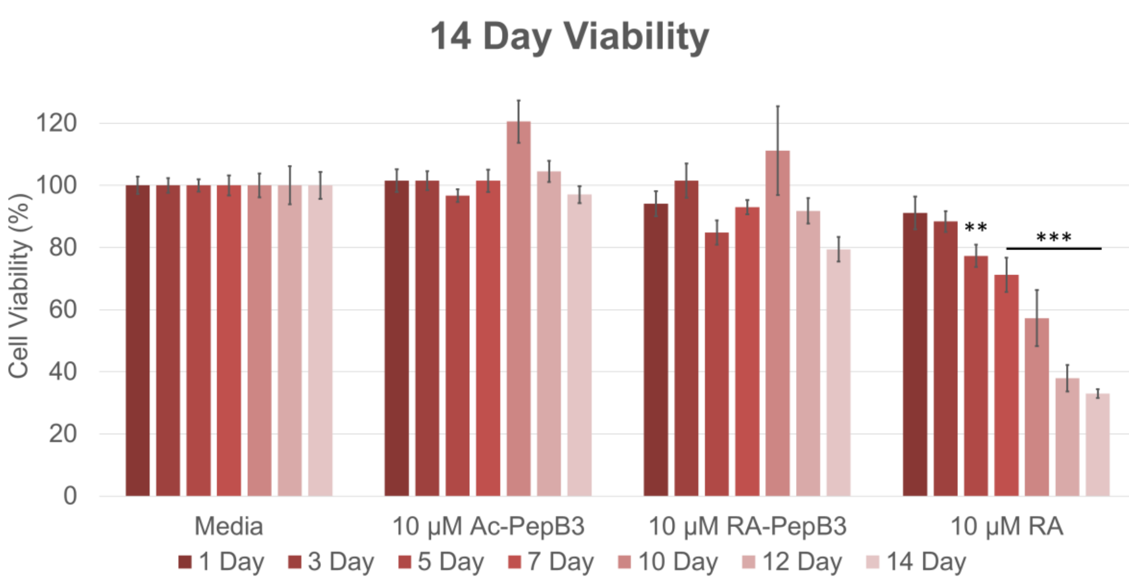

Figure 29. 14 Day Cytotoxicity Results

SH-SY5Y cytotoxicity following 14-day differentiation. No significant change in viability is detected in either of the PepB3 treatment groups, while viability of RA is decreased significantly as early as day 5. Values are represented as average ± S.E.M. N=12. Significance is reported as * ($p<0.05$), ** ($p<0.01$), or *** ($p<0.001$).

5. DISCUSSION

5.1. Peptide Physiochemical Characteristics

Two peptides were synthesized, Ac-PepB3 and RA-PepB3. The first peptide contains an acetyl group at the C-terminus, while the latter contains the treatment molecule RA. Ac-PepB3 was used to measure any effect of the peptide alone on cells, while RA-PpeB3 contained the treatment drug for delivery. Peptide samples were confirmed for successful synthesis by mass spectrometry (MS). Both peptides contain four possible sites of protonation when charged inside the mass spectrogram. Peptides become charged and samples are detected at m/z (mass per charge) of one fourth their mass. Additional ions that do not fully protonate exit at one third their mass. Both Ac-PepB3 and RA-PepB3 were successfully characterized via MS (Figure 9-10).

Peptides were additionally characterized by imaging utilizing transmission electron microscopy (TEM). Previous literature has reported that PepB3 forms a combination of α-helices and random coils that appear as a twisted structure under TEM [21]. This structure can be seen in the micrographs in Figure 11.

5.2. PepB3 & SH-SY5Y Initial Characterization

Initial experiments focused on characterizing the uptake and short-term effects of PepB3 on SH-SY5Y cells. Experiments that use RA-induced differentiation of SH-SY5Y cells typically have either a low serum media treated with 10 µM RA supplemented with BDNF (Brain-derived neurotrophic factor), or high serum media treated with 10 µM RA [11]. In order to characterize the effect of the peptide alone to induce differentiation of these cells, the later media formulation was chosen to eliminate the potential for BDNF to cause differentiation, making treatment selection the sole independent variable. Determination of a dosage for PepB3 was done by measuring its cytotoxicity up to RA's 10 μM concentration. Concentrations from 0.5 – 10 μM of both Ac-PepB3 and RA-PepB3 were tested via PrestoBlue cell viability assays, and up to a treatment of 10 μM no significant toxicity was found compared to untreated or RA treated cells. (Figure 12).

Peptide uptake was observed by fluorescence imaging of peptides following treatment. During synthesis, peptides were conjugated with a fluorophore, 5-TAMRA, that allows for a peptides location to be determined through fluorescence microscopy (Figure 13). Both Ac-PepB3 and RA-PepB3 exhibit fluorescence from the peptide localized to cells. Of these two peptides, RA-PepB3 expresses a stronger fluorescence intensity compared to Ac-PepB3. This effect is related to the amphiphilicity of each peptide. In RA-PepB3, the long hydrocarbon tail of RA creates a large hydrophobic unit that increases the overall amphiphilic strength of the peptide. This effect causes a change in the second order structures, specifically, as found in previous work, RA-PepB3 consist of 28% α-helices and Ac-PepB3 with 16% α-helices with the remaining sections forming random coils [21]. The increased order of α-helix secondary structures has been shown to play a pivotal role in the transport of peptides across the cell membrane [42].

Fluorescence images allow for identification of peptide localization but do not provide enough evidence whether the peptides have been internalized into the cell or if they are binding with the surface. To visualize internalization, Z-stack imaging was used to create a three-dimensional diagram to observe where PepB fluoresces within the cell. The strongest fluorescence is observed within the cell body adjacent the cell's nuclei, validating internalization of PepB3 by the cells (Figure 14).

5.3. SH-SY5Y Differentiation Set-up

Due to the length of the experiment conducted, the protocol went under several iterations to determine the optimal conditions for cell culture and differentiation. In normal growth media, SH-SY5Y cells will continuously proliferate with a doubling rate of 27 hours [11]. When differentiated, proliferation slows as cells change into neuron-like cells. Growing cells for a 7-day time-period using both conditions present a concern determining an optimal initial cell seeding density. For initial characterization, cells were seeded in a 96 well plate at 10,000 cells per well (31,000 cells/cm^2) and provided too little time for cells to overgrow their environment within the 24-hour time-period. When this concentration was attempted for 7 days, cells quickly overgrew the small area available and obscured neurite growth. Cells plated too low at 2,500 per well (8000 cells/cm^2) had difficulty properly growing and provided inconsistent results. A density of 5,000 cells per well (16,000 cells/cm^2) was settled on for one-week experiments, high enough to allow cells to grow properly while maintaining space for clear imaging of neurite differentiation.

In addition to modulating seeding density, the differentiation media additionally went through several iterations to reduce cell overgrowth. Serum in media was dropped from 10% FBS to 1% for 7 days. Treatments of RA and peptide were kept at 10 µM for this experiment. In reduced serum, cell viability was drastically affected after just 24 hours, and by day 7 too few cells remained to collect data. While researchers often use low serum with RA as a method to differentiate SH-SY5Y cells, it is supplemented BDNF. From this experiment, BDNF appears to play a critical role in maintaining cell viability in low serum cell populations. With the design criteria to exclude BDNF from the treatment groups, differentiation was maintained at 10% FBS.

5.4. SH-SY5Y – PepB3 Cytotoxicity

Following determination of an appropriate treatment dose, longer term treatment was performed to observe cytotoxic effects during SH-SY5Y cells differentiation into neuron-like cells. RA-induced differentiation has been reported to take up to 5 days following treatment to observe mature neuron-like cells [43]. SH-SY5Y viability was measured for 7 days to monitor cytotoxic effect during and following differentiation. Treatments doses of 1, 5, and 10 µM were used to determine if higher concentrations would have a pronounced effect over a longer time-period. For both Ac-PepB3 and RA-PepB3 at all concentrations, no significant decrease in viability was observed compared to cells cultured in proliferation media (Figure 15-16). RA treated cells at 1 and 5 µM showed no signs of toxicity over 7 days, however cells treated at 10 µM RA began showing significant toxicity at day 5, and even greater by day 7 (Figure 17). This data suggests that PepB3 does not significantly affect cell viability by itself, or with retinoic acid conjugation. In contrast, RA begins showing toxic effects by day 5, the standard time-period for cell differentiation [11], [43]. The use of PepB3 appears to improve the viability of cells during retinoic acid treatment.

5.5. SH-SY5Y Differentiation Analysis

Differentiation of SH-SY5Y cells was modeled by measurement of neurite outgrowth. Cells cultured in proliferation media maintain the morphology over the period of 7 days. As differentiation is induced, “N” type (Neuron-like) cells form and neurites extend from the cell body outward. These neurites act as an indicator for differentiation of the cells, and length of their outgrowth provides a quantitative measure towards whether cells have undergone differentiation. Measured neurites exhibit a significant difference following treatment with RA-PepB3 and RA (Figure 18-19). Untreated cells (control) do not express a significant increase in neurite length over 7 days. Both RA-PepB3 and RA neurite lengths show a significant increase by day 3 through day 7 compared to the control. Neurite lengths between the control and Ac-PepB3, and similarly RA-PepB3 and RA, exhibit no significant difference at each timepoint. These changes are also observed in micrographs for each condition during differentiation (Figure 20-23). Media and Ac-PepB3 treatment groups show cells spread out with minimal neurite extension. In the differentiation groups RA-PepB3 and RA, long neurite extensions form and branched networks begin to form between the cells.

Treatment of SH-SY5Y cells with RA has been shown to cause an increase in GAP43 expression in differentiating neurons [41]. GAP43 is a cytoplasmic protein that is expressed during neuritogenesis and has previously been found to reach peak expression following 3 days treatment of RA, after which expression returns to undifferentiated levels. This curve was observed in our experiments, with RA-PepB3 and RA treatments exhibiting a 2.5x fold increase in GAP43 expression at day 3 (Figure 24-25) before decreasing to baseline expression at day 7 (Figure 26). Analysis of cell polarity found no significant difference between control and treatment groups (Figure 27). Cells largely expressed a mix of unipolar cells and bipolar cells, consistent with previous studies [44].

5.6. Long Term Differentiation

Up to 14 days differentiation PepB3 treatments of cells did not exhibit cytotoxic effects on the cells, while RA viability dropped to 33% by day 14 (Figure 29). Neurite length analysis could not be performed on these plates due to overcrowding of culture wells. Around day 10, S-type cells began to crowd cells and by day 14 neurite became too obscured for measurements (Figure 28). While neurites presence can be seen throughout 14 days of differentiation, proliferation is not seen to cease following treatment with retinoic acid. Studies looking at differentiation of SH-SY5Y cells typically induce differentiation by coupling RA treatment with both low serum media and additional growth factors such as BDNF. RA treatment alone does

5.7. Conclusion

The work of this thesis has uncovered three key results regarding PepB3 mediated delivery of RA. PepB3 can be used to deliver retinoic acid to neuroblastomas at equal treatment doses to research investigating differentiation by freeform RA alone. This treatment has the advantage over RA of not causing a cytotoxic effect within the duration of neuroblast differentiation and can be used following mature N-type cell formation without additional effects on cell viability. Lastly, RA-PepB3 treatment can induce differentiation as measured by neurite outgrowth as effectively as standard RA treatments. The work of this thesis shows that PepB3 can be used to assist RA delivery, improve toxicity and potential for treatment.

Further peptide studies could investigate the solubility of PepB3 for understanding its absorption within the body, determination of its LC_{50} to define a maximum treatment dose, and incorporation of cell targeting peptides such RGD to increase tumor targeting or treatment. Differentiation by PepB3 may also be tested against 13cRA, the retinoic acid isomer used in clinical applications. Long term differentiation experiments could also be improved by decrease of cell seeding density followed by a longer stabilization period prior to differentiation. Differentiation studies may also look to determine changes in cell morphology following removal of PepB3 and quantify the reversibility of differentiation with this system.

REFERENCES CITED

[1] B. W. Stewart and C. P. Wild, "World Cancer Report 2014," 2014.

[2] "SEER Stat Fact Sheets: Brain and Other Nervous System Cancer," 2015. [Online]. Available: https://seer.cancer.gov/statfacts/html/brain.html. [Accessed: 23-Nov-2018].

[3] H. Korkaya and M. S. Wicha, "Selective targeting of cancer stem cells: A new concept in cancer therapeutics," *BioDrugs*, vol. 21, no. 5, pp. 299–310, 2007.

[4] H. Liu, L. Lv, and K. Yang, "Chemotherapy targeting cancer stem cells.," *Am. J. Cancer Res.*, vol. 5, no. 3, pp. 880–93, 2015.

[5] Y.-I. Jeong *et al.*, "All-trans-retinoic acid release from core-shell type nanoparticles of poly(ε-caprolactone)/poly(ethylene glycol) diblock copolymer," *Int. J. Pharm.*, vol. 273, no. 1–2, pp. 95–107, Apr. 2004.

[6] B. N. Ho, C. M. Pfeffer, and A. T. K. Singh, "Update on Nanotechnology-based Drug Delivery Systems in Cancer Treatment," *Anticancer Res.* , vol. 37, pp. 5975–5981, 2017.

[7] S. A. Castleberry, M. A. Quadir, M. A. Sharkh, K. E. Shopsowitz, and P. T. Hammond, "Polymer conjugated retinoids for controlled transdermal delivery," *J. Control. Release*, vol. 262, pp. 1–9, Sep. 2017.

[8] J. C. Gomez *et al.*, "Incorporation of Retinoic Acid Releasing Microspheres into Pluripotent Stem Cell Aggregates for Inducing Neuronal Differentiation," *Cell. Mol. Bioeng.*, vol. 8, no. 3, pp. 307–319, Sep. 2015.

[9] R. L. Carpenedo *et al.*, "Homogeneous and organized differentiation within embryoid bodies induced by microsphere-mediated delivery of small molecules," *Biomaterials*, vol. 30, no. 13, pp. 2507–2515, May 2009.

[10] C. Errico, M. Gazzarri, F. Chiellini, C. Errico, M. Gazzarri, and F. Chiellini, "A Novel Method for the Preparation of Retinoic Acid-Loaded Nanoparticles," *Int. J. Mol. Sci.*, vol. 10, no. 5, pp. 2336–2347, May 2009.

[11] J. Kovalevich and D. Langford, "Considerations for the use of SH-SY5Y neuroblastoma cells in neurobiology.," *Methods Mol. Biol.*, vol. 1078, pp. 9–21, 2013.

[12] M. Rhinn and P. Dollé, "Retinoic acid signalling during development," *Development*, vol. 139, no. 5, pp. 843–858, May 2012.

[13] K. Venkatesh *et al.*, "In vitro differentiation of cultured human CD34+ cells into astrocytes.," *Neurol. India*, vol. 61, no. 4, pp. 383–8, 2013.

[14] C. Rochette-Egly, “Retinoic acid signaling and mouse embryonic stem cell differentiation: Cross talk between genomic and non-genomic effects of RA,” *Biochim. Biophys. Acta - Mol. Cell Biol. Lipids*, vol. 1851, no. 1, pp. 66–75, Jan. 2015.

[15] S. Yu, L. Levi, R. Siegel, and N. Noy, “Retinoic acid induces neurogenesis by activating both retinoic acid receptors (RARs) and peroxisome proliferator-activated receptor β/δ (PPARβ/δ).,” *J. Biol. Chem.*, vol. 287, no. 50, pp. 42195–205, Dec. 2012.

[16] B. H. Kushner, S. Modak, E. M. Basu, S. S. Roberts, K. Kramer, and N.-K. V. Cheung, “Posterior reversible encephalopathy syndrome in neuroblastoma patients receiving anti-G_{D2} 3F8 monoclonal antibody,” *Cancer*, vol. 119, no. 15, pp. 2789–2795, Aug. 2013.

[17] J. Louisse, S. Gönen, I. M. C. M. Rietjens, and M. Verwei, “Relative developmental toxicity potencies of retinoids in the embryonic stem cell test compared with their relative potencies in in vivo and two other in vitro assays for developmental toxicity,” *Toxicol. Lett.*, vol. 203, no. 1, pp. 1–8, May 2011.

[18] J. A. Palmer *et al.*, “A human induced pluripotent stem cell-based in vitro assay predicts developmental toxicity through a retinoic acid receptor-mediated pathway for a series of related retinoid analogues,” *Reprod. Toxicol.*, vol. 73, pp. 350–361, Oct. 2017.

[19] M. Schroeder and C. Zouboulis, “All- *trans* -Retinoic Acid and 13- *cis* -Retinoic Acid: Pharmacokinetics and Biological Activity in Different Cell Culture Models of Human Keratinocytes,” *Horm. Metab. Res.*, vol. 39, no. 2, pp. 136–140, Feb. 2007.

[20] E. Z. Szuts and F. I. Harosi, “Solubility of retinoids in water,” *Arch. Biochem. Biophys.*, vol. 287, no. 2, pp. 297–304, Jun. 1991.

[21] W. Ma *et al.*, “A Novel Cell Penetrating Peptide for the Differentiation of Human Neural Stem Cells,” *Biomolecules*, vol. 8, no. 3, p. 48, Jul. 2018.

[22] A. D. Frankel and C. O. Pabo, “Cellular uptake of the tat protein from human immunodeficiency virus,” *Cell*, vol. 55, no. 6, pp. 1189–1193, Dec. 1988.

[23] M. Green and P. M. Loewenstein, “Autonomous functional domains of chemically synthesized human immunodeficiency virus tat trans-activator protein,” *Cell*, vol. 55, no. 6, pp. 1179–1188, Dec. 1988.

[24] E. Vivès, P. Brodin, and B. Lebleu, “A truncated HIV-1 Tat protein basic domain rapidly translocates through the plasma membrane and accumulates in the cell nucleus.,” *J. Biol. Chem.*, vol. 272, no. 25, pp. 16010–7, Jun. 1997.

[25] S. Y. Choi *et al.*, “Mutational analysis of a human immunodeficiency virus type 1

Tat protein transduction domain which is required for delivery of an exogenous protein into mammalian cells," *J. Gen. Virol.*, vol. 83, no. 5, pp. 1173–1181, May 2002.

[26] A. Joliot, C. Pernelle, H. Deagostini-Bazin, and A. Prochiantz, "Antennapedia homeobox peptide regulates neural morphogenesis.," *Proc. Natl. Acad. Sci. U. S. A.*, vol. 88, no. 5, pp. 1864–8, Mar. 1991.

[27] D. Derossi, M. H. Joliot, G. Chassaing, and A. Prochiantz, "The Third Helix of the Antennapedia Homeodornain Translocates through Biological Membranes," *J. Biol. Chem.*, vol. 269, no. 14, pp. 10444–10450, 1994.

[28] G. Guidotti, L. Brambilla, and D. Rossi, "Cell-Penetrating Peptides: From Basic Research to Clinics.," *Trends Pharmacol. Sci.*, vol. 38, no. 4, pp. 406–424, Apr. 2017.

[29] W. Ma and W. H. Suh, "Engineered cell penetrating peptides," in *ACS Symposium Series*, vol. 1271, 2017, pp. 297–319.

[30] S. Futaki *et al.*, "Arginine-rich peptides. An abundant source of membrane-permeable peptides having potential as carriers for intracellular protein delivery.," *J. Biol. Chem.*, vol. 276, no. 8, pp. 5836–40, Feb. 2001.

[31] M. C. Morris, S. Deshayes, F. Heitz, and G. Divita, "Cell-penetrating peptides: from molecular mechanisms to therapeutics," *Biol. Cell*, vol. 100, no. 4, pp. 201–217, Apr. 2008.

[32] J. Oehlke *et al.*, "Cellular uptake of an α-helical amphipathic model peptide with the potential to deliver polar compounds into the cell interior non-endocytically," *Biochim. Biophys. Acta - Biomembr.*, vol. 1414, no. 1–2, pp. 127–139, Nov. 1998.

[33] J. Oehlke, E. Krause, B. Wiesner, M. Beyermann, and M. Bienert, "Extensive cellular uptake into endothelial cells of an amphipathic β-sheet forming peptide," *FEBS Lett.*, vol. 415, no. 2, pp. 196–199, Sep. 1997.

[34] Kristen Sadler, Khee Dong Eom, Jin-Long Yang, and Yoana Dimitrova, and J. P. Tam*, "Translocating Proline-Rich Peptides from the Antimicrobial Peptide Bactenecin 7†," 2002.

[35] M. Rhee and P. Davis, "Mechanism of uptake of C105Y, a novel cell-penetrating peptide.," *J. Biol. Chem.*, vol. 281, no. 2, pp. 1233–40, Jan. 2006.

[36] C.-Y. Jiao, D. Delaroche, F. Burlina, I. D. Alves, G. Chassaing, and S. Sagan, "Translocation and endocytosis for cell-penetrating peptide internalization.," *J. Biol. Chem.*, vol. 284, no. 49, pp. 33957–65, Dec. 2009.

[37] J. P. Richard *et al.*, "Cell-penetrating peptides. A reevaluation of the mechanism of

cellular uptake.," *J. Biol. Chem.*, vol. 278, no. 1, pp. 585–90, Jan. 2003.

[38] J. L. Biedler, L. Helson, and B. A. Spengler, "Morphology and Growth, Tumorigenicity, and Cytogenetics of Human Neuroblastoma Cells in Continuous Culture1," 1973.

[39] M. M. Shipley, C. A. Mangold, and M. L. Szpara, "Differentiation of the SH-SY5Y Human Neuroblastoma Cell Line.," *J. Vis. Exp.*, no. 108, p. 53193, Feb. 2016.

[40] R. A. McCloy, S. Rogers, C. E. Caldon, T. Lorca, A. Castro, and A. Burgess, "Partial inhibition of Cdk1 in G_2 phase overrides the SAC and decouples mitotic events," *Cell Cycle*, vol. 13, no. 9, pp. 1400–1412, May 2014.

[41] T. Kumea *et al.*, "Dibutyryl cyclic AMP induces differentiation of human neuroblastoma SH-SY5Y cells into a noradrenergic phenotype," *Neurosci. Lett.*, vol. 443, no. 3, pp. 199–203, Oct. 2008.

[42] M. Okuyama *et al.*, "Small-molecule mimics of an α-helix for efficient transport of proteins into cells," *Nat. Methods*, vol. 4, no. 2, pp. 153–159, Feb. 2007.

[43] M. Encinas *et al.*, "Sequential Treatment of SH-SY5Y Cells with Retinoic Acid and Brain-Derived Neurotrophic Factor Gives Rise to Fully Differentiated, Neurotrophic Factor-Dependent, Human Neuron-Like Cells," *J. Neurochem.*, vol. 75, no. 3, pp. 991–1003, Jan. 2002.

[44] R. Filograna *et al.*, "Analysis of the Catecholaminergic Phenotype in Human SH-SY5Y and BE(2)-M17 Neuroblastoma Cell Lines upon Differentiation.," *PLoS One*, vol. 10, no. 8, p. e0136769, 2015.

APPENDIX A:

ABBREVIATIONS

13cRA	13-cis Retinoic Acid
ATRA	All-trans Retinoic Acid
CPP	Cell-Penetrating Peptide
CTCF	Corrected Total Cell Fluorescence
D10FPS	DMEM w/ 10% Fetal Bovine Serum + 1% Pen/Strep
DIC	Differentiation Interference Contract Microscopy
GAP43	Growth Associated Protein – 43
HPLC	High Performance Liquid Chromatography
ICC	Immunocytochemistry
MS	Mass Spectrometry
NB	Neuroblastoma
NLS	Nuclear Localization Signal
N-Type Cells	Neuron-Like Cells
RA	All-trans Retinoic Acid
SPPS	Solid Phase Peptide Synthesis
S-Type Cells	Surface Adherent Epithelial-Like Cells
TAMRA	5-Carboxytetramethylrhodamine
TAT	Trans-Activator of Transcription
TEM	Transmission Electron Microscopy